

Books/Book Chapters/Conference Papers 2016-17

SI No.	Name of the Teacher	Title of the book/ chapters published	Title of the Paper	Title of the proceedings of the conference	Name of the conference	National/ International	Year of publication	ISBN/ISSN number of the proceeding	Affiliating Institute at the time of publication	Name of the Publisher
1	V.R. Sastry and G. Raghu Chandra	NexGen Technologies for Mining & Fuel Industries	Tapping of Electrical Energy from Ground Vibrations caused due to Blasting – An Innovation			International	18 SEPTEMBER S2017	ISBN: 978-93-85926-40-2	National Institute of Technology Karnataka, Surathkal	Allied Publishers
2	M Krishna Murthy		Reduction in loss of data packets and performance comparison of improvise DSR Protocol	7th International Conference on Recent Engineering & Technology	7th International Conference on Recent Engineering & Technology	International	7th April 2017	ISBN 978-81-904760-9-6		
3	Vedala Rama Sastry and Garimella Raghu Chandra		Signal Processing Computation based Seismic Energy Estimation of Blast induced Ground Vibration Waves	2016 IEEE Distributed Computing, VLSI, Electrical Circuits and Robotics (DISCOVER)	IEEE – International Conference on Distributed Computing, VLSI, Electrical Circuits and Robotics (DISCOVER)	International	13-14 August 2016	ISBN: 978-1-5090-1623-5/16	National Institute of Technology, Karnataka, Surathkal	IEEE
4	Lakshmi, K., Pusalatha, D.V., Naidu, A.S.K. and Singh, S. K		Hybrid Neural Network - Genetic Algorithm for Prediction of Mechanical Properties of ASS-304 at Elevated Temperatures	5th International conference on Materials Processing and Characterization (ICMPC), 12-13 March		International	12-13 March 2017		Methodist College of Engg and Tech., Hyd	
5	Vuppu Padmakar		Emperical Analysis of Software Security Engineering - Phase wise	1st National Conference on Convergence of Emerging Technologies in Computer Science & Engineering (CETCSE-2K17)	1st National Conference on Convergence of Emerging Technologies in Computer Science & Engineering (CETCSE-2K17)	National	22-23 Feb 2017		Visveshvaraya College of Engg. & Technology	Visveshvaraya College of Engg. & Technology
6	Vuppu Padmakar		User Interface Development - An Research Scope	1st National Conference on Convergence of Emerging Technologies in Computer Science & Engineering (CETCSE-2K17)	1st National Conference on Convergence of Emerging Technologies in Computer Science & Engineering (CETCSE-2K17)	National	22-23 Feb 2017		Visveshvaraya College of Engg. & Technology	Visveshvaraya College of Engg. & Technology
7	Dr.G.Aravind		FC and ZFC Magnetic properties of Ferro-spinels (MFe2O4) prepared by Solution- Combustion method	International Conference on Functional materials, Characterization, Solid State Physics, Power, Thermal and Combustion Energy FCSPTC Conference-2017	International Conference on Functional materials, Characterization, Solid State Physics, Power, Thermal and Combustion Energy FCSPTC Conference-2017	International	7-8 April 2017	DOI: 10.1063/1.4990232	Methodist college of Engineering and Technology	NA
8	John William Carey M		“Single lead EEG acquisition system for health care applications,” (Scopus Cited)	proceedings of the 2016 IEEE International Conference on Inventive Computation Technologies	ICICT 2016	INTERNATIONAL	26-27 August 2016			
9	Dr.B.Krishna Kumar		Performance Comparison Of Various Thresholding Techniques On The Removal Of Ocular Artifacts In The EEG Signals	IEEE Conference , International Conference on Inventive Computation Technologies	ICICT2016	INTERNATIONAL	26-27 August 2016		GNITC	IEEE CONFERENCE PROCEEDINGS
10	Lavanya Pamulaparty		A Gradient Boosting Approach for large-scale Network Parameter Configuration In Big Data“	International Conference on “Recent Innovations in Engineering and Technology”	International Conference on “Recent Innovations in Engineering and Technology”	International	22-23 DECEMBER 2016			

PRINCIPAL
METHODIST COLLEGE OF ENGG. & TECH.
 King Koti Road, Abids, Hyderabad

NxGenMiFu-2017

NexGen Technologies for Mining and Fuel Industries



**Pradeep K Singh
V K Singh
A K Singh
D Kumbhakar
M P Roy**
Editors



75 Years of

CSIR Touching Lives

ALLIED PUBLISHERS PRIVATE LIMITED

1/13-14 Asaf Ali Road, **New Delhi**–110002

Ph.: 011-23239001 • E-mail: delhi.books@alliedpublishers.com

87/4, Chander Nagar, Alambagh, **Lucknow**–226005

Ph.: 0522-4012850 • E-mail: appltldko9@gmail.com

17 Chittaranjan Avenue, **Kolkata**–700072

Ph.: 033-22129618 • E-mail: cal.books@alliedpublishers.com

15 J.N. Heredia Marg, Ballard Estate, **Mumbai**–400001

Ph.: 022-42126969 • E-mail: mumbai.books@alliedpublishers.com

60 Shiv Sunder Apartments (Ground Floor), Central Bazar Road,
Bajaj Nagar, **Nagpur**–440010

Ph.: 0712-2234210 • E-mail: ngp.books@alliedpublishers.com

F-1 Sun House (First Floor), C.G. Road, Navrangpura,
Ellisbridge P.O., **Ahmedabad**–380006

Ph.: 079-26465916 • E-mail: ahmbd.books@alliedpublishers.com

751 Anna Salai, **Chennai**–600002

Ph.: 044-28523938 • E-mail: chennai.books@alliedpublishers.com

Hebbar Sreevaishnava Sabha, Sudarshan Complex-2

No. 24/1, 2nd Floor, Seshadri Road, **Bangalore**–560009

Ph.: 080-22262081 • E-Mail: bngl.books@alliedpublishers.com

3-2-844/6 & 7 Kachiguda Station Road, **Hyderabad**–500027

Ph.: 040-24619079 • E-mail: hyd.books@alliedpublishers.com

Website: www.alliedpublishers.com

© 2017, NexGen Technologies for Mining and Fuel Industries

No part of the material protected by this copyright notice may be reproduced or utilized in any form or by any means, electronic or mechanical including photocopying, recording or by any information storage and retrieval system, without prior written permission from the copyright owners. The views expressed in this volume are of the individual contributors, editor or author and do not represent the view point of the Centre.

ISBN: 978-93-85926-40-2

Published by Sunil Sachdev and printed by Ravi Sachdev at Allied Publishers Pvt. Ltd., (Printing Division), A-104 Mayapuri Phase II, New Delhi-110064

Committees

PATRONS

Dr. Girish Sahni
DG, CSIR & Secretary, DSIR, New Delhi

Shri Gurdeep Singh
Chairman, NTPC, New Delhi

Shri Rahul Guha
DG, DGMS, Dhanbad

Shri Sutirtha Bhattacharya
Chairman, Coal India Limited, Kolkata

CHAIRMAN, ORGANISING COMMITTEE

Dr. Pradeep K Singh
Director, CSIR-CIMFR, Dhanbad

ORGANISING SECRETARY

Dr. V.K. Singh
Chief Scientist, CSIR-CIMFR, Dhanbad

CONVENER

Dr. A.K. Singh
Sr. Principal Scientist, CSIR-CIMFR, Dhanbad

CO-CONVENERS

Shri D. Kumbhakar
Principal Scientist, CSIR-CIMFR, Dhanbad

Dr. M.P. Roy
Principal Scientist, CSIR-CIMFR, Dhanbad

INTERNATIONAL COMMITTEE

Prof. J.A. Sanchidrian
Univ. Politecnica de Madrid, Spain

Prof. William L. Fourney
University of Maryland, USA

Prof. Bibhu Mohanty
University of Toronto, Canada

Dr. William Adamson
Austin Power International, Chile

Prof. Enrique Munaretti
Univ. Federal do Rio Grande do Sul, Brazil

Prof. Dr. Carsten Drebenstedt
TU Bergakademie, Freiberg, Germany

Prof. Xuguang Wang
China Society of Engg. Blasting, China

Prof. Peter Moser
University of Leoben, Austria

Dr. Ewan Sellers
JK Tech, Australia

Dr. A.T. Spathis
Orica Mining Services, Australia

Dr. Petr Konicek
Institute of Geonics, Czech Republic

Prof. John Coggan
Camborne School of Mines, UK

Prof. Sarma S. Kanchibotla
University of Queensland, Australia

Prof. Colin D. Hills
University of Greenwich, London, UK

NATIONAL COMMITTEES

Steering Committee

Shri N. Sridhar

CMD, SCCL, Hyderabad

Shri Ch. Venkaiah Chowdary

Vice Chairman & Managing Director, APMDC

Dr. R.K. Sinha

Controller General, IBM, Nagpur

Shri Sunil Duggal

CEO, Hindustan Zinc Limited, Udaipur

Prof. A.K. Ghose

Former Director, Indian School of Mines, Dhanbad

Prof. D.P. Singh

Emeritus Professor, IIT (BHU), Varanasi

Prof. B.B. Dhar

Former Director, CMRI, Dhanbad

Shri Gopal Singh

CMD, CCL, Ranchi

Shri T.K. Nag

CMD, NCL, Singrauli

Shri R.R. Mishra

CMD, WCL, Nagpur

Shri Anil Kumar Jha

CMD, MCL, Sambalpur

Shri Shekhar Sharan

CMD, CMPDI, Ranchi

Shri B.R. Reddy

CMD, SECL, Bilaspur

Dr. A. Sinha

Former Director, CSIR-CIMFR, Dhanbad

Prof. D.C. Panigrahi

Director, IIT (ISM), Dhanbad

Dr. K. Muraleedharan

Director, CSIR-CGCRI, Kolkata

Shri C.K. Asnani

CMD, UCIL, Jaduguda

Shri M. Chaudhari

CMD, MOIL, Nagpur

Shri A.K. Khurana

DG, APP, New Delhi

Shri Sarat Kumar Acharya

CMD, NLC, Neyveli

Shri C.K. Dey

CMD, ECL, Sanctoria

Shri Avijit Ghosh

CMD, HEC, Ranchi

Shri Akhilesh Joshi

President, International Business, HZL, Udaipur

Shri Rajeev Singhal

VP (Raw materials), Tata Steel

Shri G.K. Satish

Director (P&BD), Indian Oil Corporation Ltd.

Advisory Committee

Shri L.S. Shekhawat

COO, Hindustan Zinc Limited, Udaipur

Dr. V. Venkateswarlu

Director, NIRM, Bangalore

Prof. A.K. Singh

IIT (ISM), Dhanbad

Prof. Ashis Bhattacharjee

IIT, Kharagpur

Prof. V.R. Sastry

NIT, Karnataka, Surathkal

Prof. K. Srinivas

Anna University, Chennai

Prof. M.P. Singh

Banaras Hindu University, Varanasi

Shri A. Manohar Rao

Director (P&P), SCCL, Hyderabad

Shri D. Gongopadhyay

Director (P&P), BCCL, Dhanbad

Shri S. Chandra

Director (P&P), CCL, Ranchi

Shri A.K. Mishra

Director (P&P), CCL, Ranchi

Shri Binay Dayal

Director (T/P&D), CMPDI, Ranchi

Shri B.N. Shukla

Director (Op), ECL, Sanctoria, West Bengal

Shri A.K. Singh

Director (P&P), ECL, Sanctoria, West Bengal

Prof. P.S. Dixit
IIT (Banaras Hindu University), Varanasi

Prof. G.K. Pradhan
AKS University, Satna

Shri S.I. Hussain
Dy. DG, DGMS, SC Zone, Hyderabad

Shri P.K. Sarkar
Dy. DG, DGMS, HQ, Dhanbad

Shri Utpal Saha
Dy. DG, DGMS, Eastern Zone, Sitarampur

Shri B.P. Ahuja
Dy. DG, DGMS, North-Western Zone, Udaipur

Dr. A.K. Sinha
Dy. DG, DGMS, South Eastern Zone, Ranchi

Shri R. Kulshetra
Dy. DG, DGMS, Northern Zone, Ghaziabad

Shri S. Krishnamurthy
Dy. DG, DGMS, Western Zone, Nagpur

Shri D.B. Naik
Dy. DG (Elec), DGMS, HQ, Dhanbad

Shri G.L. Kanta Rao
Dy. DG (Mech), DGMS, HQ, Dhanbad

Shri A.K. Jha
Director (Tech.), NTPC Limited, New Delhi

Shri K.K. Sharma
Director (O), NTPC Limited, New Delhi

Dr. N.K. Nanda
Director (Tech), NMDC, Hyderabad

Shri Raman
Director (Tech.), SAIL

Dr. Saibal K. Gupta
Director, JSW Steel Ltd.

Dr. R.K. Malhotra
DG, Petroleum Fed. of India, New Delhi

Shri B. Ramesh Kumar
Director (O), SCCL, Hyderabad

Shri O.P. Singh
Director (P&P), MCL, Sambalpur, Odisha

Shri J.P. Singh
Director (Op), MCL, Sambalpur, Odisha

Shri G. Pandey
Director (Op), NCL, Singrauli, MP

Shri J.L. Singh
Director (P&P), NCL, Singrauli, MP

Shri K. Prasad
Director (Op), SECL, Bilaspur, Chhattisgarh

Shri P.K. Sinha
Director (P&P), SECL, Bilaspur, Chhattisgarh

Shri B.K. Mishra
Director (Op), WCL, Nagpur

Shri T.N. Jha
Director (P&P), WCL, Nagpur

Shri A.D. Sao
COO, IDL Explosives Ltd.

Shri A.K. Tailor
Director (Tech), MPPGCL, Jabalpur

Shri Kapil Dhagat
Sr. VP, JSPL, New Delhi

Shri Subir Das
Director (Mines), NLC, Neyveli

Shri P. Selvakumar
Director (P&P), NLC, Neyveli

Shri P.S. Mishra
Director, OMDC, Kolkata

Shri H.D. Nagaraja
Executive Director, APMDC

Shri Bhola Singh
Project Director, Sasan Power Limited, MP

Shri S. Menon
Sr. GM, Solar Industries India Ltd, Nagpur

Shri Manish Sinha
GM (Explosives), Indian Oil Corporation Ltd.

Dr. H.S. Venkatesh
National Institute of Rock Mechanics, Bangalore

Reviewers

Dr. T.N. Singh
Dr. Amalendu Sinha
Dr. Pradeep K Singh
Dr. Pijush Pal Roy
Shri Ashim Choudhury
Shri Achyut Krishna Ghosh
Dr. S. Majumder
Prof. U.K. Dey
Dr. V.K. Singh
Dr. R.K. Goel
Dr. Rajendra Singh
Dr. Gautam Banerjee
Dr. Chandra Nath Ghosh
Dr. A. Kushwaha
Dr. R.V.K. Singh
Dr. N. Sahay
Dr. Ashis Mukherjee
Dr. S.K. Mandal
Dr. T. Gouricharan
Shri T.B. Das
Dr. V.K. Kalyani
Dr. R.C. Tripathi
Dr. Ashok Kumar Singh
Dr. Shripal Singh
Dr. S.K. Roy
Dr. R.K. Tiwari
Dr. R.S. Singh
Dr. Bably Prasad
Dr. Sudipto Datta
Dr. A.K. Raina
Dr. M.R. Saharan
Dr. John L.P.
Dr. V.A. Mendhe
Dr. More Ramulu
Shri D. Kumbhakar
Dr. Kumar Nikhil
Dr. Abhay Kumar Singh
Dr. Lalan Kumar
Dr. S. Maity
Dr. N.K. Srivastava
Dr. C. Sawmliana
Dr. S.N. Nandi
Dr. P.D. Chavan
Dr. K.M.K. Sinha
Dr. S.K. Ray
Dr. Pinaki Sarkar
Dr. U.S. Chattopadhyay
Dr. Manoj Kumar Sethi
Dr. M.P. Roy
Dr. Siddharth Singh
Dr. Manish Kumar
Dr. Harsh Verma
Dr. P.K. Mishra
Dr. R.E. Masto
Dr. Ajay Kumar Singh
Dr. A. Prakash
Dr. K.M.P. Singh
Dr. M.K. Saini
Dr. Ranjan Kumar
Dr. N.K. Mohalik
Dr. D. Mohanty
Dr. Ashis K. Ghosh
Dr. S.K. Chaulya
Dr. Gajanan Sahu
Dr. G.K. Bayen

Preface

Efficient management and sustainable development are two key elements, which need to be addressed for optimal utilization of natural resources. The challenges for development of mining and fuel sectors include scientific mining, conservation and proper utilization of low grade mineral resources, clean coal initiatives, management of mining waste and above all, the environmental protection. In Indian scenario, coal is the mainstay of the energy mix. Hence, it is equally important to address the issues related to efficient and optimum utilization of coal as well as exploitation of alternative cleaner fuels.

An International Conference on “NexGen Technologies for Mining and Fuel Industries” is, therefore, being organized during February 15–17, 2017 at Vigyan Bhawan, New Delhi by CSIR-Central Institute of Mining and Fuel Research, Dhanbad, India to deliberate on the subject among the stake holders.

The proceedings of the conference, in two volumes, include the contributions from authors across the globe on the latest research in mining and fuel technologies, focussing on:

- *Innovative Mining Technology*, highlighting novel ideas for futuristic developments in mining.
- *Rock Mechanics and Stability Analysis*, covering both laboratory and field evaluation of rock characterisation and stabilisation based on modern mechanics approaches.
- *Advances in Explosives and Blasting*, dealing with the recent developments in the field of explosives and blasting with special emphasis on rock fragmentation.
- *Mine Safety and Risk Management*, stressing upon the global and regional safety evaluation techniques in mining areas and importance of risk assessment.
- *Computer Simulation and Mine Automation*, describing the application of advanced numerical modelling techniques for design optimisation and mechanisation in mining.
- *Natural Resource Management for Sustainable Development*, discussing recovery from low grade ores and wastes with emphasis on better conservation and sustainability.
- *Environmental Impacts and Remediation*, narrating the impact evaluation and mitigating techniques for environmental protection.
- *Paste Fill Technology and Waste Utilisation*, covering utilization of waste for mine filling and reclamation.
- *Fly Ash Management*, dealing with utilisation and value addition of fly ash through various means.
- *Clean Coal Initiatives*, discussing judicious and scientific utilisation of coal vis-a-vis clean coal technologies.

- *Mineral Processing and Coal Beneficiation*, talking about recent developments in processing of coal and minerals for gainful utilisation.
- *Quality Coal for Power Generation*, narrating the role of coal quality for improved coal-fired power generation.
- *Conventional and Non-conventional Fuels and Gases*, including recent developments in the area of alternative fuels.

I, along with my co-editors gratefully acknowledge the help and co-operation we have received from all the members of the International as well as National Steering, Advisory and Organising Committees. The authors have immensely added value to the proceedings, for which we are indebted to them. Our sincere acknowledgements are due to the researchers who have critically peer-reviewed all the submissions, which greatly helped to maintain high standard of the publication. The services of M/s KW Conferences are also thankfully acknowledged.

Lastly, organizing an event of this magnitude, as NxGnMiFu-2017, would not have been possible without the generous financial support by our sponsors, to whom we owe a debt of gratitude.

I wish all our distinguished guests, participants and colleagues, attending this international event, a very fruitful and joyous stay at New Delhi.

February, 2017
New Delhi

Pradeep K Singh

Tapping of electrical energy from ground vibrations caused due to blasting: An innovation

V.R. Sastry and G. Raghu Chandra

Department of Mining Engineering, National Institute of Technology, Karnataka, Surathkal, India

ABSTRACT: Generation of electrical energy has become a basic aspect in power system, because of increasing demands from citizenry in electrical distribution system. Power may be generated in different ways. Numerous developments took place in power generation technology for the generation of electricity, but those are all dependent on conventional sources. In the present research, generation of electrical energy using piezo sensors was done by tapping electrical voltage from undesirable ground vibrations generated from blasts in mines.

Blasting operations in mines and quarries always result in ground vibrations, which are of major environmental concern. Studies were carried out in three different limestone mines and two different sandstone formations of coal mines, situated in Southern India, to assess and analyze the seismic energy resulting from the blast induced ground vibrations. In total, 116 blast vibration events in limestone formation and 94 blast vibration events in sandstone formation were studied from various blasts. It was observed that there is a potential for tapping of electrical energy from the ground vibrations generated due to blasts carried out in mines and quarries, using piezo sensors. Piezo generator circuits were developed and used in addition to the seismographs at different distances, from short to long range, in all mining locations, to tap the ground vibrations. Electrical voltage was tapped from the blast induced ground vibrations during studies, which later was used for running low powered VLSI systems as ambient power source. Also, it was noticed that the obtained electrical potential is in direct proportion to the input vibration intensity.

The range of voltage tapped from ground vibrations is up to 4531.42 mV in limestone and 4277.51 mV in sandstone formations. Further, the amount of voltage acquired was used to obtain the intensity of blast vibrations. A very good correlation between seismic energy (obtained from ground vibrations using signal processing analysis) and electrical energy (obtained from piezo generator developed) was observed during the studies. Results also indicated that the working of piezo sensor in tapping ground vibrations is as accurate as conventional ground vibration monitors.

1. INTRODUCTION

When the explosive charge detonates in a blasthole under confinement, the chemical energy of the explosive is converted into heat and works to the surroundings with an enormous pressure according to the first principle of thermodynamics (Johansson and Persson^[1]). Explosion of a spherical charge in an infinite rock medium results in three major zones: (1) Explosion cavity, where explosion energy is

liberated and the process is hydrodynamic; (2) Transition zone, where plastic flow, crushing and cracking occur; and (3) Seismic zone, where strain waves travel as seismic waves (Atchison *et al.*,^[2] Nicholls,^[3] Sastry^[4]).

Partitioning of explosive energy in a blast depends on the end effects involved. For instance, part of the fracture work is in its first stage intimately connected to the shock wave flow in the locality of the hole and, in later

stages, also to the rock movement, which begins as the fractures burst open. All other energy transfer takes place obviously, as follows: (a) expansion work of the fractures, that is absorbed as elastic and plastic deformation of rock in the surface of fractures as they are penetrated by the gases; (b) heat transferred to the rock from hot detonation products; and (c) heat and work conveyed as enthalpy of the gases venting to the atmosphere through open fractures and stemming (Sanchidria'n *et al.*^[5]).

Seismographs, high-speed video camera and fragmentation monitoring systems are used to measure the seismic field, initial velocity of the blasted rock face and the fragment size distribution, respectively, from which various energy terms are calculated.

2. PIEZO-GEN TECHNIQUE

Piezoelectricity is a phenomenon of electricity assembled in some solid materials (such as crystalline particles, certain ceramic substances, and biological composition for example—bone, DNA and various proteins) due to applied mechanical stress. Electricity resulting from applied pressure is known as piezoelectricity. The word “piezo” derived from the Greek “piezein”, means to squeeze or press, and “electric” or “electron”, derived from “amber”, which is an ancient source of electric charge. Piezoelectricity was discovered in 1880 by French physicists Jacques and Pierre Curie (Anon,^[6] Jacques and Curie;^[7] Tingley^[8]).

Piezoelectricity is the ability of some materials such as crystals and certain ceramics, to generate an electric potential in response to applied mechanical stress or heat (Jacques and Curie;^[7] Pramethesth and Ankur^[9]). However, piezoelectricity is not caused by a change in charge density on the surface, but by dipole density in the bulk. For example, a 1 cm³ cube of quartz with 2 kN of applied force can produce a voltage of 12,500 V (Jacques and Curie^[10]). Mechanical compression or tension on a poled piezoelectric ceramic element changes the dipole moment, creating a voltage. Compression along the direction of polarization, or tension perpendicular to the direction of polarization, generates voltage of the same polarity as the poling voltage (Figure 1).

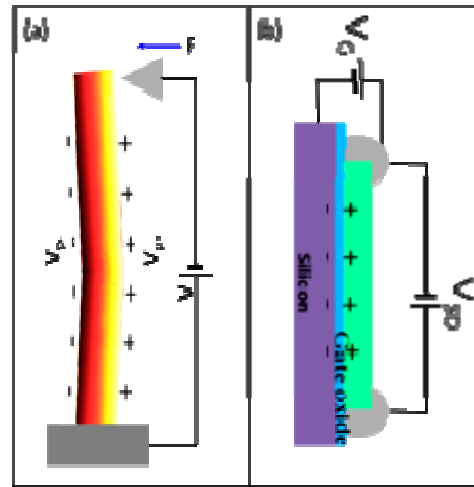


Fig. 1. Working mechanism of simple piezo transducer (Anon^[11]).

3. VIBRATION MONITORING AND RECORDING INSTRUMENTS (SEISMOGRAPHS)

Many types of seismographs are available today. Each performs the basic function of measuring ground motion, but supplies much additional information. Most seismographs are equipped with meters that register and hold the maximum value of the vibration components and sound level. Other seismographs are equipped to produce a printout which gives a variety of information such as maximum value for each component, frequency of vibration for the maximum value, maximum displacement, maximum acceleration, vector sum, and sound level. Blast information such as date, blast number, time, location, job designation, and other pertinent information can also be added to the printout (Konya and Walter^[12]).

4. SEISMIC ENERGY

Energy transferred into the strata in the form of seismic waves is calculated as an integral of the energy flow past a control surface at a given distance from the blast. Energy flux (power or rate of energy dissipated per unit area) is the scalar product of the stress at the surface and the particle velocity (Achenbach^[13]). Calcula-

tions of seismic energy and its comparison with explosive energy have been reported by many researchers like Howell and Budenstein,^[14] Fogelson *et al.*,^[15] Berg and Cook,^[16] Nicholls,^[17] Atchinson,^[18] and more recently by Hinzen.^[19] Berta^[20] attempted to use some of the energy concepts in his principles of blast design. The seismic energy dissipated by a ground vibration event at a given distance from blast site could be a critical component in assessing performance of blasts.

5. ASSESSMENT OF SEISMIC ENERGY

5.1 Ground vibrations monitoring

Intensity of ground vibrations generated due to blasting operations was monitored using three units of Minimate Plus, InstanTel, Canada. These ground vibration monitors are of 8-Channelled instruments with six channels recording three mutually orthogonal ground vibration components, namely Transverse, Vertical and Longitudinal at two locations. The fourth and eighth channels record noise level using microphone. Minimates with geophones and microphones connected are placed at different distances covering both short and long range distances, from the blast site. The vibration events were later transferred to a computer using advanced blastware software. Using the full wave forms, the seismic energy was estimated for all the signals in three directions, based on the principle that the area within the curve is 'Seismic Energy Dissipated' using DADiSP Signal Processing software. Care was taken to filter the noise.

DADiSP is a signal processing tool/software, using which shock energy dissipated in the form of waves is calculated. Longitudinal, Transverse and Vertical components of blast vibration events were imported from blastware software to digital signal processing software DADiSP in ASCII format. Fast Fourier Transformation was performed subsequently to find the frequency component of the time domain of blast wave signal as blast wave recorded by Minimate Plus and processed by Blastware falls in the category of random progressive

signal. The estimation of absolute area describes the intrinsic energy of the blast wave signal distributed in various frequency bands. The energy of the signal $x(t)$ is given by $\int_{-\infty}^{\infty} [|x(t)|]^2 dt$ (Sastry^[21]).

6. FIELD INVESTIGATIONS AND RESULTS

Blasts were carried out in various mines for the extraction and assessment of seismic energy. Ground vibration monitors were placed near blast field at various distances to find the impact of blast on nearby structures. Geophones were glued to the ground with the help of Plaster of Paris for proper contact. The piezo generator circuits were placed beside the conventional seismographs for maintaining accuracy in the obtained data. In total, 55 blasts were analyzed for the assessment of seismic energy based on electrical energy generation technique, out of which 10 blasts were carried out in Choutapalli limestone mine, 11 blasts were carried out in Yepalamadhavaram limestone mine and 34 blasts were carried out in coal mines of The Singareni Collieries Company Ltd. The following are some photographs depicting obtained electricity from undesirable seismic waves, extracted through piezo-gen circuit in various mine locations (Figure 2).

Seismic data collected at various distances from different blasts were compared with the obtained electrical energy data as shown in Tables 1 and 2.



Fig. 2(a). Piezo-Gen circuit.



Fig. 2(b). Extraction of electricity using piezo-gen circuit from undesirable blast vibrations.



Fig. 2(c). Observation of obtained voltage from the blast vibrations undesirable by multimeter for the assessment of seismic energy.

Table 1. Summary of seismic energy extracted as electricity from blasts conducted in limestone mines

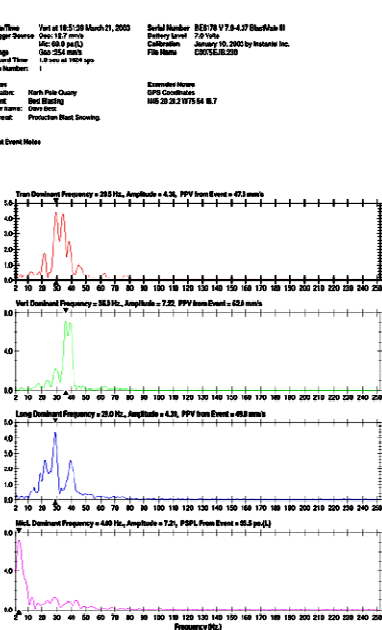
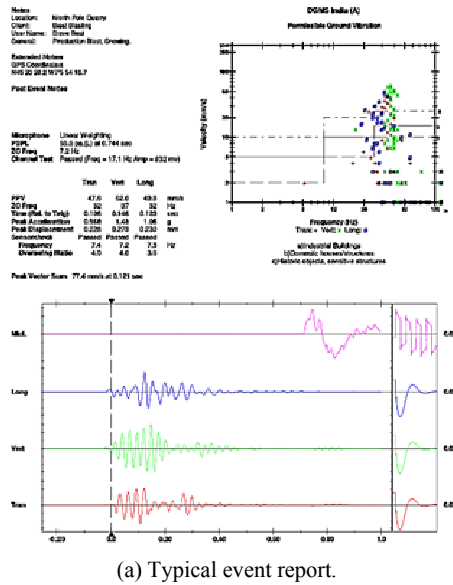
Sl. no.	Distance (m)	MCD (kg)	PPV (mm/s)	Seismic energy from three mutually orthogonal ground vibrations (MJ)	Electrical energy extracted from blast vibrations (MJ)
1	30	38.33	64.4	42256215	4509139.6
2	40	38.33	39.2	18524598	1963630.3
3	45	38.33	37.5	17108152	1709115.6
4	50	38.33	26.3	6729443	299095.23
5	55	38.33	22.5	14013633	1526210.7
6	60	38.33	11.8	6377533	248069.74
7	40	37.5	55.6	26656654	2424915.1
8	50	37.5	35.6	11103330	1041516.2
9	55	37.5	29.3	5419536	234614.75
10	60	37.5	27.3	3903284	103863.11
11	65	37.5	26.4	18419851	1634399
12	65	37.5	22.7	7523677	460683.92
13	50	70.14	61	25837627	2571913.8
14	65	70.14	41.9	13666773	1407946
15	65	70.14	39.4	9824630	833789.96
16	70	70.14	32.5	2895806	64473.335
17	40	36.57	40	6548821	283286.87
18	50	36.57	30.1	4453486	123605.68
19	55	36.57	28.2	3232849	88722.367
20	70	36.57	16.1	712081	16118.334
21	75	36.57	10.4	964048	18693.452
22	80	36.57	3.43	306033	1931.3388
23	40	39.06	32.2	6893020	326396.26
24	50	39.06	28.2	6264554	243229.47

Sl. no.	Distance (m)	MCD (kg)	PPV (mm/s)	Seismic energy from three mutually orthogonal ground vibrations (MJ)	Electrical energy extracted from blast vibrations (MJ)
25	80	39.06	2.41	156568	95.374756
26	134	39.06	11.7	359719	3433.4912
27	40	39.28	171	59727766	7186831.2
28	50	39.28	181	99699604	11691266
29	55	39.28	68.8	27009086	3014047.3
30	75	39.28	10.3	2040307	40081.241
31	80	39.28	38.6	28970681	3120027.8
32	85	39.28	7.75	1901915	36266.251
33	50	51.4	118	21503717	2142627.3
34	60	51.4	126	111259278	13291238
35	65	51.4	91.4	58338415	6943699.5
36	90	51.4	38.1	5758561	262356.88
37	95	51.4	30.9	24691269	3269370.3
38	100	51.4	12.3	3366361	88722.367
39	30	24.58	44.7	23418621	2961119.1
40	38	24.58	42	38133182	4654974.8
41	50	24.58	23.7	9264400	633502.97
42	90	24.58	19.8	3331585	88722.367
43	95	24.58	18.4	4060162	110253.22
44	100	24.58	15	6492304	348280
45	40	14.35	34.8	3185760	80210.17
46	50	14.35	14.4	627148	13733.965
47	75	14.35	8.76	473566	8607.5717
48	80	14.35	8.13	240986	1168.3408
49	85	14.35	6.73	446799	6103.9844
50	40	30.36	34.4	12451737	1122775.5
51	50	30.36	23.1	8552912	550884.59
52	60	30.36	14.6	5350973	168241.07
53	70	30.36	11	1241977	24415.938
54	40	28.33	37.6	14565085	1699792.7
55	45	28.33	35.4	12675683	1164549.6
56	55	28.33	23.1	8573518	572844.63
57	70	28.33	15.5	4502870	137721.15

Table 2. Summary of seismic energy extracted as electricity from blasts conducted in coal mine

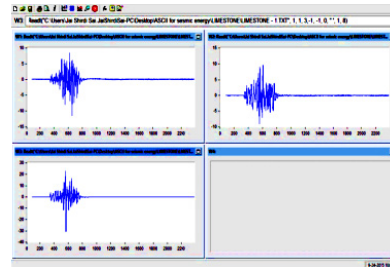
Sl. no.	Distance (m)	MCD (kg)	PPV (mm/s)	Seismic energy from three mutually orthogonal ground vibrations (MJ)	Electrical energy extracted from blast vibrations (MJ)
1	100	66	53.5	2738832.38	547766.476
2	110	66	33.8	1511665.32	151166.532
3	120	66	29.3	1470468.86	147046.886
4	150	66	18.92	6916156.65	4841309.66
5	160	66	17.4	5245447.1	3147268.26
6	170	66	17.3	8461652.43	7615487.19
7	184	50	5.33	1562458.55	1249966.84
8	178	88	22.61	9277651.8	7422121.44
9	188	88	20.2	4747405.68	2373702.84
10	200	88	17.9	366544.54	36654.454
11	292	88	4.06	376992.65	188496.325
12	150	85	19.81	10544797.7	10544797.7
13	209	85	10.7	2280225.67	456045.134
14	234	85	8.89	1055142.78	105514.278
15	295	85	3.3	134876.62	53950.648
16	696	450	3.56	513484.49	205393.796
17	719	450	1.52	136859.22	82115.532
18	750	450	1.52	171645.3	102987.18
19	800	450	1.02	1.836	1.836
20	603	460	7.11	1980472.55	594141.765
21	636	460	2.29	160142.93	112100.051
22	678	460	1.9	166647.59	66659.036
23	721	460	1.27	45698.08	45698.08
24	220	100	9.4	8769781.29	9646759.42
25	380	100	1.4	172599.58	172599.58
26	1591	1953	1.02	79583.75	79583.75
27	1856	1953	0.89	71031.38	71031.38
28	2033	1953	0.89	49481.5	49481.5
29	2121	1953	0.63	1.134	1.134
30	304	90	3.43	638174	638174
31	332	90	2.67	164876	98925.6
32	379	90	1.14	61901.33	111422.394
33	280	100	4.32	615873.463	123174.693
34	290	100	2.92	73406.109	44043.6654
35	300	100	2.03	402677.92	402677.92
36	440	100	1.27	108396.33	108396.33

Typical sample event report and FFT reports generated from the blastware software are shown in Figure 3. Seismic energy was obtained from the events recorded using signal processing tool, DADiSP. Sample of signal processing window is shown in Figure 4.

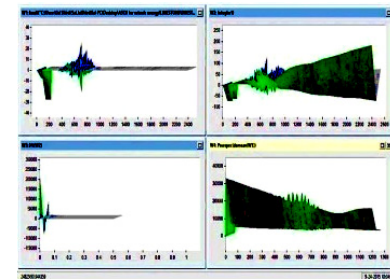


(b) Typical FFT report from blastware.

Fig. 3. Screenshots of vibration events recorded by minimate plus.



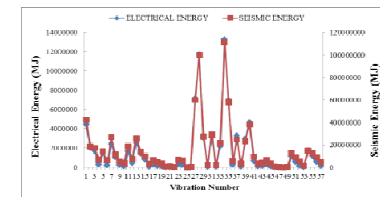
(a) Signal processing window



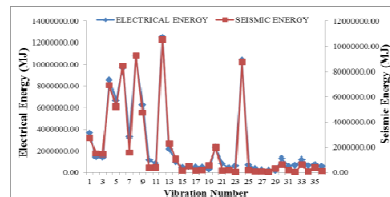
(b) Estimation of seismic energy.

Fig. 4. Finding of shock energy dissipated using DADiSP.

Also, comparison of seismic energy with the generated electrical energy was made to observe the amount of undesirable vibrations which were converted to electricity (Figure 5). From the analysis, it was observed that amount of seismic energy extracted in the form of Electricity is 80–90% of the total seismic energy in limestone mines and that is about 75–80% in the case of coal mines.



(a) In limestone mines.



(b) In coal mine.

Fig. 5. Amount of electrical Energy extracted from blast induced vibrations with its corresponding seismic energy in various blasts.

7. CONCLUSIONS

Based on the study, the following conclusions are drawn:

- Studies indicated that the amount of seismic energy increased with increase in maximum charge per delay. Hence, the optimal usage of MCD improves the performance of blasts by reducing seismic energy loss and improving explosive energy utilization.
- Seismic waves in the form of ground vibrations induced due to blasts can be efficiently tapped and converted with the help of Piezo-Gen circuit into useful electrical energy.
- The amount of seismic energy obtained in case of limestone mines is higher than in coal mines.
- The Piezo-Gen circuit may become a renewable source for generation of electricity from ground vibrations caused by blasting operations and further will be more useful in assessing the seismic energy in blast field.

REFERENCES

- [1] Johansson, C.H. and Persson, P.A. (1970). *Detonics of high Explosives* (Academic Press: London).
- [2] Atchison, T.C., Duvail, W.I. and Pugliese, J.M. (1964). Effect of decoupling on explosion generated strain pulses in rock (USBM RI: 6333).
- [3] Nicholls, H.R. (1962). "Coupling explosive energy to rock" *Jl. of Geophysics*, 27(3), 305–16.
- [4] Sastry, V.R. (1989). A study into the effect of some parameters on rock fragmentation by blasting, Ph.D. Thesis, BHU, India.
- [5] Sanchidrian Jose' A., Segarra Pablo and Lina M. Lopez (2007). Energy components in rock blasting, *International Journal of Rock Mechanics and Mining Sciences*, 44, 130–147.
- [6] Anon (2015). All About Heaven, web Site <http://www.allaboutheaven.org/science/149/121/piezoelectricity> (accessed on 28 August, 2015).
- [7] Jacques and Pierre Curie (1880). On electric polarization in hemihedral crystals with inclined faces, 91, 383–386.
- [8] Tingley, R. (2013). "Method and application of piezoelectric energy harvesting as a mobile power source", Research and Design Project, New Hampshire.
- [9] Pramethesth, T. and Ankur, S. (2013). Piezoelectric Crystals: Future Source of Electricity, *International Journal of Scientific Engineering and Technology*, 2(4), 260–262.
- [10] Jacques and Pierre Curie, 1881. Contractions and expansions produced by voltages in hemihedral crystals with inclined faces, 93, 1137–1140.
- [11] Anon, 2016. "Piezotronics", web link <https://en.wikipedia.org/wiki/Piezotronics>, (accessed on Sept. 14, 2016).
- [12] Konya, C.J. and Walter, E.J. (1990). *Surface Blast Design* (Prentice Hall Publishers: USA).
- [13] Achenbach, J.D. (1975). "Wave propagation in elastic solids. Amsterdam." *Elsevier*, 166.
- [14] Howell, B.F. and Budenstein, D. (1955). "Energy distribution in explosion generated seismic pulses", *Geophysics*, 20(1), 33–52.
- [15] Fogelson, D.E., Atchison, T.C. and Duvall, W.I. (1959). "Propagation of peak strain and strain energy for explosion-generated strain pulses in rock." *Proc. of the 3rd US Symp. on Rock Mechanics, Colorado School of Mines*, Golden, 271–284.
- [16] Berg, J.W. and Cook, K.L. (1961). "Energies, magnitudes and amplitudes of seismic waves from quarry blasts at Promontory and lakeside, Utah." *Seismol Soc. Bull.*, 51(3), 389–400.
- [17] Nicholls, H.R. (1962). "Coupling explosive energy to rock", *Geophysics*, 27(3), 305–316.
- [18] Atchinson, T.C. (1968). "Fragmentation principles." in: Pfeleider EP, editor. *Surf Mining*. New York: The American Institute of Mining, *Metallurgical and Petroleum Engineers*, 355–72.
- [19] Hinzen, K.G. (1998). "Comparison of seismic and explosive energy in five smooth blasting test rounds." *Int. J Rock Mech Min Sciences*, 35(7), 957–67.
- [20] Berta, G. (1990). "L esplosivostrumento di lavoro". *Milan: Italesplosivi*, 31–64.
- [21] Sastry, V.R. (2014). "Assessment of Performance of Explosives/Blast results based on Explosive Energy Utilization", *Unpublished R&D Project Report, submitted to Coal India Limited*.

7TH INTERNATIONAL CONFERENCE ON RECENT ENGINEERING & TECHNOLOGY 2017

ORGANIZED BY
ORGANIZATION OF SCIENCE & INNOVATIVE ENGINEERING AND TECHNOLOGY, CHENNAI



IN ASSOCIATION WITH
MATRUSRI ENGINEERING COLLEGE, HYDERABAD

Approved by AICTE & Affiliated to Osmania University

Certificate of Presentation

This is to certify that
Dr./Mr./Ms. M.V.D.S. Krishna Murthy
from NMREC, Hyderabad
for his/her presented in

7TH INTERNATIONAL CONFERENCE ON RECENT ENGINEERING & TECHNOLOGY 2017
(07th April 2017)

Paper Titled

REDUCTION IN LOSS OF DATA PACKETS AND
PERFORMANCE COMPARISON OF THE IMPROVISED
DSR PROTOCOL


Secretary


Director

Signal Processing Computation based Seismic Energy Estimation of Blast induced Ground Vibration Waves

Vedala Rama Sastry (*Author*)
Professor: Department of Mining Engineering
 National Institute of Technology Karnataka,
 Surathkal, INDIA
 vedala_sastry@nitk.edu.in

Garimella Raghu Chandra* (*Author*)
Research Scholar: Department of Mining Engineering
 National Institute of Technology Karnataka,
 Surathkal, INDIA
 graghuchandra_mn14f02@nitk.edu.in*

Abstract—Study of ground vibrations resulted from blasting operations in mines and quarries is significant ecological aspect. In general, very lesser amount of explosive energy will be utilized in blasting process for breakage and creation of fragmentation, however the remaining will be squandered in the form of shock waves. Shock waves resulted from blasting operations cannot be entirely abolished, nonetheless can be lessened to the extent possible using an appropriate blasting methodology. Substantial work has been performed to detect ground vibrations for assessing the blast performance using the intensity of ground vibrations. Nevertheless, not much research has carried in the estimation of seismic energy and utilizing this energy for assessing the performance of blast rounds. In this paper, a Signal Processing based technique for the estimation of seismic energy dissipated at various distances is proposed. In total, 116 blast vibration events from Limestone Mines, 96 blast vibration events from Underground Coal Mine and 43 blast vibration events from Sandstone Mines were collected and respective signal processing analysis was carried out using Advanced Blastware and DADISP software. Each vibration event in one direction carries about 2500 particle motion samples.

Keywords—*Blast Vibrations, Seismic Energy, Signal Processing Approach, DADISP, Advanced Blastware, Discrete Fourier Transformation (DFT), Power Spectrum Density, Angular Momentum, Rotational Kinetic Energy*

I. INTRODUCTION

When the explosive charge detonates in a blasthole under confinement, the chemical form of explosive energy is converted into gases and work to the surroundings with an enormous pressure according to the first principle of thermodynamics. Explosion of a spherical charge in an infinite rock medium result in three major zones (Fig. 1): (1) Explosion cavity - where explosion energy is liberated and the process is hydrodynamic; (2) Transition zone - where plastic flow, crushing and cracking occur; and (3) Seismic zone - where strain waves travel as seismic waves [4][7][9].

The partition of the explosive energy in a blast depends on the end effects involved. For instance, part of the fracture work is in its first stage intimately

connected to the shock wave flow in the locality of the hole and, in the later stages, also to the rock movement, which begins as the fractures burst open. All other energy transfer takes place obviously, as follows: (a) expansion work of the fractures, that is absorbed as elastic and plastic deformation of the rock in the surface of the fractures as they are penetrated by the gases; (b) heat transferred to the rock from the hot detonation products; and (c) heat and work conveyed as enthalpy of the gases venting to the atmosphere through open fractures and stemming [8].

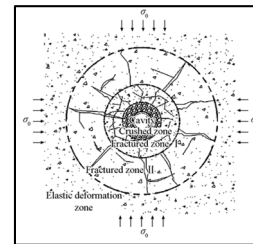


Fig. 1 Zones of rock deformation around a blasthole [4]

Therefore, the energy balance of the blast can thus be expressed by:

$$EE = EF + ES + EK + ENM$$

where,

EE	=	Explosive energy
EF	=	Fragmentation energy
ES	=	Seismic energy
EK	=	Kinetic energy
ENM	=	Energy forms not measured

Research studies carried out have indicated that in opencast mines there is a potential of seismic energy generation from 2-13J from a given blast. Also studies have indicated possible correlation between maximum charge per delay and the seismic energy. Therefore, a study leading to the possible estimation of energy dissipated at different distances from the blast site may be of industrial utility [11].

Seismic waves are classified as body waves and surface waves. Body waves travel through the interior of earth. Ground vibration waves are of two

types, Primary (P-wave) and Secondary (S-wave). Surface waves generate when the radiating body waves impinge on a stress free plane, like surface or any discontinuity. These waves travel along the surface and discontinuities. Rayleigh waves are the best known surface waves and include both dilation and distortion of the medium. Surface waves carry maximum percentage of the radiated energy and are predominant at longer distances from the blast source, since their attenuation rate is slower than body waves. In addition, the frequency of surface waves is lower than body waves and frequently found to be in the range most favorable for structural response [5]. All these waves are characterized by exponential decrease in particle oscillation amplitude as distance from energy source increases [12]. Fig. 2 shows the characteristics of ground vibration waves on the structures.

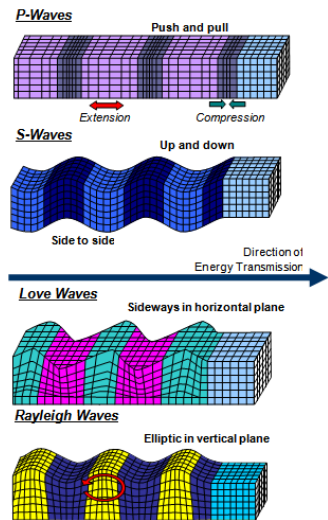


Fig. 2 Characteristics of Body Waves and Surface Waves

Vibration monitoring and recording instruments (Seismographs)

Many types of seismographs are available today. Each performs the basic function of measuring ground motion but supplies much additional information. Most seismographs are equipped with meters that register and hold the maximum value of the vibration components and the sound level. Other seismographs are equipped to produce a printout which gives a variety of information such as maximum value for each component, frequency of vibration for the maximum value, maximum displacement, maximum acceleration, vector sum, and sound level. Blast information such as date, blast number, time, location, job designation, and other pertinent information can also be added to the printout [6].

Normally, a seismograph record shows the following information (Fig. 3):

- Three lines or traces, one for each vibration component. A fourth line or trace for the acoustic or sound level.
- A calibration signal for each trace.
- Timing lines which appear as vertical lines running across all or part of the record.

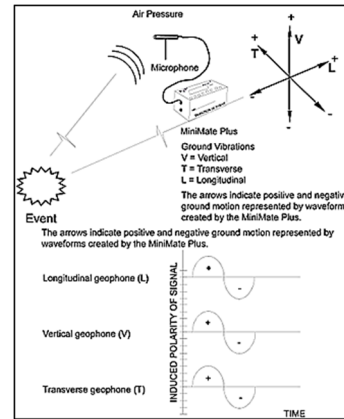


Fig. 3 A Seismograph record [3]

From the studies conducted by previous research [10], it is found that the actual utilization of explosive energy for the productive work is about 15-20%, and remaining energy is wasted in the form of unwanted side effects like ground vibrations. If the energy utilization could be improved even by 1%, there would be huge benefits to the industry, with much reduced environmental effects. In this paper, an attempt for the estimation of shock wave energy through the analysis of ground vibration waves generated from the blasts conducted in mines was made using signal processing techniques, in order to determine the energy carried / dissipated, later to be used in optimizing the blast design process.

II. FIELD INVESTIGATIONS

Initially for the assessment and estimation of seismic energy, blasts were conducted in three different mine formations in Southern part of India viz. Limestone, Underground Coal and Sandstone. For Signal Processing Analyses purpose, in total 116 blast vibration event samples were collected in three different Limestone Mines by conducting 32 opencast mine blast studies. Similarly, 96 blast vibration event samples were collected from Underground Coal Mine by conducting 34 blast studies. Further, 43 blast vibration event samples were collected in two different Sandstone Mines by conducting 16 opencast mine blast studies.

In Limestone formation, the distance between the monitoring point of vibration monitor (or seismograph) and blast site was varied from 30m to 485m. In Underground Coal formation, the vibration monitor (or seismograph) was placed both on surface (with about 65m parting) and in underground for

finding the exact propagation of blast wave. The distance between vibrations monitor and blast location was varied from 15m to 111m in underground and from 54m to 122m on surface. Similarly, in Sandstone formation, the distances of monitoring instrument were varied as 100m to 2033m from the blast location.

III. RESEARCH METHODOLOGY

Vibrations induced from blasting operations were monitored using Ground Vibration Monitors. Ground vibrations generated from all the blasts were monitored at different distances and at specific structures using Microprocessor based Blast Vibration Monitors of InstanTel, Canada. The geophone of the monitor was glued to the structure / ground with Plaster of Paris for effective tapping of ground vibration wave by geophone. Typical monitoring of ground vibrations is shown in Fig. 4. A typical wave form obtained is shown in Fig. 5. The typical vibration event samples were analyzed using Advanced Blastware Software.



Fig. 4 Ground vibrations monitoring at different locations during blast studies

The obtained vibration event samples data from Vibration Monitors were analyzed with the help of Advanced Blastware and DADiSP software using signal processing techniques. Initially, the vibration samples of ground vibration events were converted into ASCII file using Advanced Blastware. The vibrations were analyzed using signal processing techniques available in the Advanced Blastware and found the intensity of blast waves (Fig. 6). The obtained ASCII values were imported into DADiSP for further signal processing analyses.

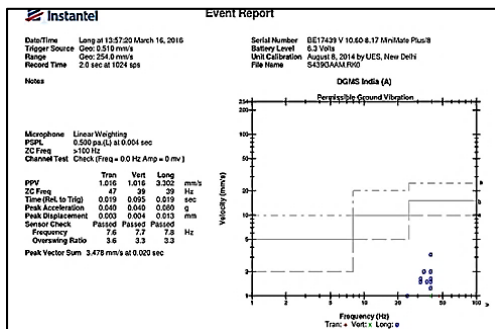


Fig. 5 Typical ground vibration event

Seismic energy can be obtained by considering area under the combination of three orthogonal vibration waves in frequency response.

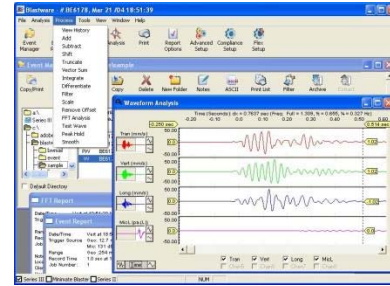


Fig. 6 Signal Processing Analysis of a blast vibration using Advanced Blastware

Initially, the discrete ASCII samples of Vibration wave obtained from Advanced Blastware are imported in DADiSP for reconstruction of Vibration wave which gives rise to quantized discrete signal (Fig. 7). At about 2500 vibration samples were recorded for a vibration in one direction and similarly vibrations in other two orthogonal directions were recorded with about 2100-2500 particle motion samples.

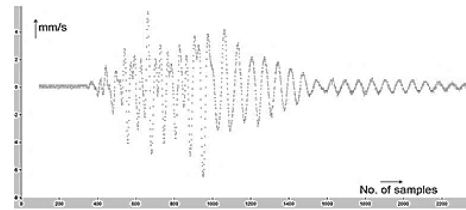


Fig. 7 Quantized discrete signal

The vibration samples were further processed to obtain a reconstructed vibration wave using reconstruction signal analysis available in DADiSP software in steps (Fig. 8). After the reconstruction process, the reconstructed sampled blast induced vibration analog waves were taken considering all three orthogonal directions for further signal processing computation (Fig. 9).

The waveforms which were in time domain were converted to frequency domain by applying Discrete Fourier Transformation (DFT). Since, Blast wave is a non-periodic discrete wave, application of direct Fourier Transformations for finding the frequency is not possible. Application of Discrete Fourier Transformation remains the system magnitude with same units but in frequency domain (Fig. 10).

This indicates no change in the state of the signal. After DFT using DADiSP package, the signals were further processed to find Power Spectrum Density. Power Spectral Density (PSD) is a measure of a signal's power intensity in the frequency domain. In practice, the PSD is computed from the DFT spectrum of a signal. The PSD provides a useful way to characterize the amplitude versus frequency content of a random signal [2].

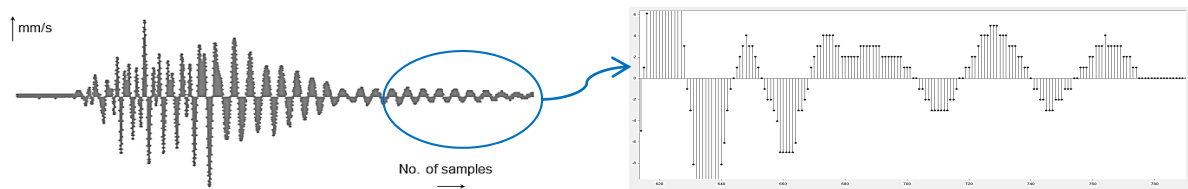


Fig. 8A Signal with discrete sample magnitudes

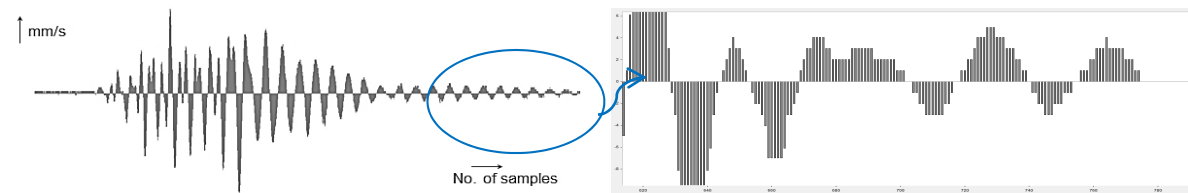


Fig. 8B Reconstruction of a signal with discrete samples

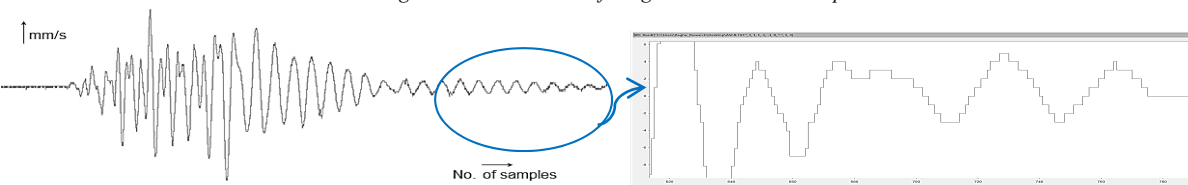


Fig. 8C Reconstructed quantized signal

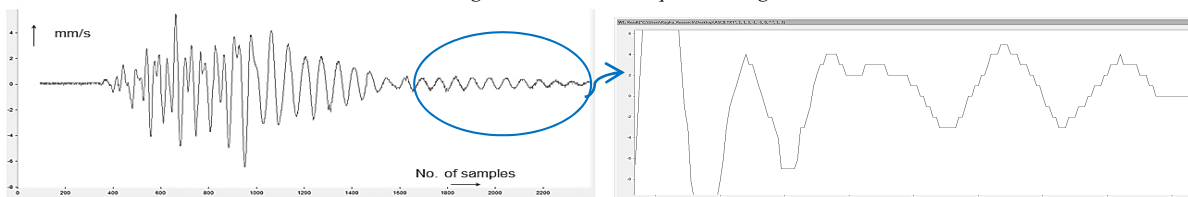


Fig. 8D Reconstructed discrete signal

Fig. 8 Reconstruction of Discrete Samples using DADiSP Package

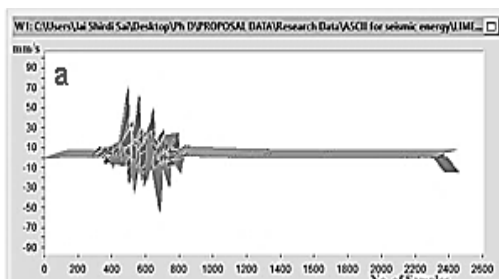


Fig. 9 Typical reconstructed vibration wave in three orthogonal directions

- Input (before DFT) – Vibration Velocity in time domain (mm/s)
- Output (after DFT) – Vibration Velocity in frequency domain (mm/s)

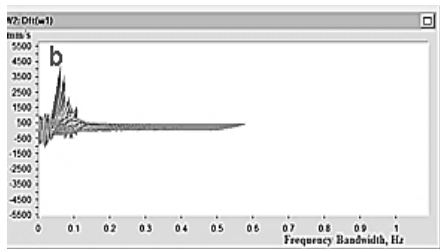


Fig. 10 Computation of DFT to random vibration signal aligned in three directions

When the input random vibration signal in frequency domain having units as 'G', the amplitude values of a PSD are normally expressed in 'G²/Hz', where the term 'G' indicates units of the random vibration signal, mm/s, in frequency domain (Fig. 11). Therefore, application of PSD to the vibration signal gives rise to,

- Input (before PSD) – Vibration Velocity in frequency domain (mm/s)
- Output (after PSD) – (mm/s)²/Hz → (μm²/s²)/Hz → μm²/s

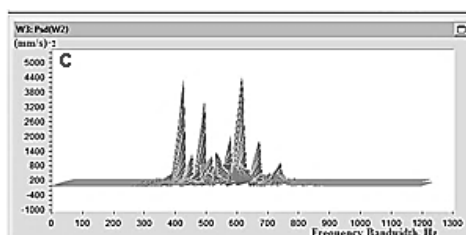


Fig. 11 Computation of Power Spectrum Density to the random vibration signal aligned in three directions after DFT operation

It was assumed that the vibration wave had a unit mass, M in kg. Therefore, the output after PSD operation was changed as μ (kg.m²/s). Output is in the form of angular momentum (L). The angular

momentum, L of a rigid body with moment of inertia I rotating with angular velocity ω , is given by:

$$L = I.\omega$$

where,

L = Angular momentum, $\text{kg}\cdot\text{m}^2/\text{s}$

I = Moment of inertia, $\text{kg}\cdot\text{m}^2$

ω = Angular Velocity, rad/s

The Rotational Kinetic Energy for a mechanical system considering the total mechanical energy of a rigid body is defined as,

$$KE_r = \int_0^\omega L d\omega = \int_0^\omega (I.\omega) d\omega = \frac{1}{2} I.\omega^2$$

where,

KE_r = Rotational Kinetic Energy, μ . Joules

Hence, from the above analysis, it is needed to apply integration to the output of vibration data after PSD operation. Since, Integration is applied only for continuous signals and for discrete signals application of integration is not possible. Hence, “Partial Sum” operation is computed for finding the Rotational Kinetic Energy available in the waveform [1]. Then the area under the vibration waves after “Partial Sum” were calculated which gives rise to the **Seismic Energy** of the blast induced vibration wave by using the command `area(abs(w4))`, which returns the area under the signal, seismic energy, at the left side bottom of the window (Fig. 12).

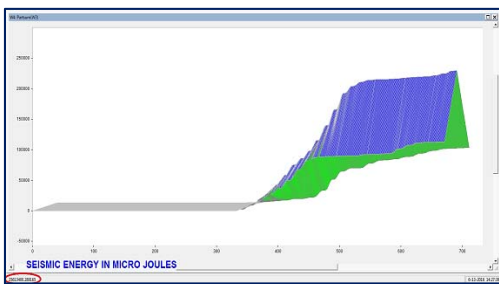


Fig. 12 Seismic Energy of the blast induced vibration wave

IV. CONCLUSIONS

From the studies conducted and analysis computed, the following conclusions are drawn:

- Analysis done in three different rock formations indicated that, the coefficient of determination, R^2 , between Seismic Energy and Peak Particle Velocity is higher in the case of sandstone formation (about 95.19%) compared to the other two formations, with limestone formation of about 90.00%, coal formation of about 91.94%. This designates that there is a direct relationship between Seismic Energy and vibration intensity. Higher is the vibration intensity amplitude, more will be the seismic energy value.

- From the regression analysis made, it was observed that there is a proper correlation between Seismic Energy and Scaled Distance in all three different rock formations. In limestone formation it is about 83.92%, in coal formation it is about 81.76% and in sandstone formation it is about 85.68%.
- The minimum and maximum values of Seismic energies in three formations are 26762 μJ and 111259278 μJ , in Limestone formation, 4250 μJ and 1904089 μJ , in Coal formation, and 10311 μJ and 27388321 μJ , in Sandstone formation.
- The range of L-wave and T-wave velocities are 120m/s to 5,275m/s and 92m/s to 4,289m/s, respectively in Limestone formation, 79.44m/s to 10,10,800m/s and 1.19m/s to 1,01,080m/s, respectively in Coal formation and 109.05m/s to 75,000m/s and 108.70m/s to 20,000m/s, respectively in Sandstone formation.
- From the results, the velocity of ground vibrations is found to be lesser in case of limestone formation, which may be due to more discontinuities. Also it indicates relatively better utilization of explosive energy.

REFERENCES

- [1] Anon, (1997). “Rotational Kinetic Energy”, website <http://theory.uwinnipeg.ca/physics/rot/node6.html> (accessed on October 19, 2015).
- [2] Anon, (2015). “PSD (Power spectral density) - description by Brüel & Kjær”, (accessed on June 6, 2015).
- [3] Anon, (2015). Minimate Plus Operator Manual, InstanTel, Canada.
- [4] Leng Zhendong, Lu Wenbo, Chen Ming, Yan Peng, Hu Yingguo, (2014). “A new theory of rock-explosive matching based on the reasonable control of crushed zone”, ENGINEERING, Vol. 12, Issue: 6, 32-38.
- [5] Holloway, R., Lundborg, N., and Runquist, G., (1983). “Ground vibrations and damage criteria”, SWEDEFO Report R85:1981.
- [6] Konya, C.J., and Walter, E.J., (1990). Surface blast design, Prentice Hall Publishers, USA.
- [7] Nicholls, H.R., (1962). “Coupling explosive energy to rock”, Geophysics, 27(3), 305–316.
- [8] Sanchidrian, J.A., Segarra, P., and Lina, M.L., (2007). “Energy components in rock blasting”, International Journal of Rock Mechanics & Mining Sciences, 44, 130–147.
- [9] Sastry, V.R., (1989). “A study into the effect of some parameters on rock fragmentation by blasting”, Unpublished Ph.D. Thesis, BHU, India.
- [10] Sastry, V.R., (2001). “Study of the effect of ground vibrations and fly rock caused due to blasting operations in Kallakudi limestone mine”, An Unpublished Technical Report submitted to Dalmia Cement (Bharat) Limited, Tamilnadu
- [11] Sastry, V.R., and Ramchandrar, K., (2014). “Assessment of performance of explosives / blast results based on explosive energy utilization”, Unpublished R&D Project Report, Central Mine Planning and Design Institute Ltd., Ranchi, India.
- [12] Taquieddin, S.A., 1982. “The role of borehole containment on surface ground vibration levels at closed scaled distances”.



5th International Conference on Materials Processing and Characterization (ICMPC 2016)

A Hybrid Neural Network - Genetic Algorithm for Prediction of Mechanical Properties of ASS-304 at Elevated Temperatures

Lakshmi Kanumuri^{a,*}, D V Pushpalatha^b, Akshay S.K. Naidu^c Swadesh Kumar Singh^c

^a*Department of CSE, GRIET, Hyderabad-500090, Telangana, India*

^b*Department of EEE, GRIET, Hyderabad-500090, Telangana, India*

^c*Department of CIVIL ENGINEERING, IARE, Hyderabad-500090, Telangana, India*

^d*Department of MECHANICAL ENGINEERING, GRIET, Hyderabad-500090, Telangana, India*

Abstract

In the present work, genetic algorithm is implemented, to optimize the artificial neural networks used, to predict the mechanical properties of Austenitic Stainless Steel 304 (ASS-304) at elevated temperatures. ASS-304 is a very important alloy used in various applications involving high temperatures which make it very important to study the mechanical properties at elevated temperatures. The dynamic neural networks have been employed first for predicting the mechanical properties such as Ultimate Tensile Strength (UTS), Yield Strength (Ys), % elongation, Strain Hardening Exponent (n) and Strength Coefficient (K) at elevated temperatures. Genetic algorithm was then integrated with the neural network model for optimization, to achieve better regression statistics, taking the mean square error as the fitness function. The results show that the proposed hybrid, neural network - genetic model is more accurate and effective method for predicting the mechanical properties of ASS-304 at elevated temperatures.

© 2017 Published by Elsevier Ltd.

Selection and peer-review under responsibility of the Conference Committee Members of the 5th International conference on Materials Processing and Characterization (ICMPC 2016)

Keywords: ASS-304; Material Properties; Artificial Neural Network; Genetic Algorithm

1. Introduction

Austenitic Stainless Steel is very important alloy used in various high temperature applications, include: as fuel cladding, core structural elements in nuclear industries due its high corrosion resistance in seawater environment because of the addition of molybdenum which prevents chloride corrosion[1]. Since it has very less carbon content,

* Corresponding author. Tel.: +91-9000005181;

E-mail address: lakshmi.kanumuri@yahoo.com.

wear resistance, friction properties are adequate in the heat effected zone and during welding there is very less susceptibility to intergranular corrosion[2]which make it important to study their mechanical properties at elevated temperatures[3].Austenitic stainless steels (300-series), when subjected to high temperatures and loads, there is a martenstic transformation involved plastic deformation which depends on several parameters: chemical composition, mechanical stress and magnetic behavior[4].The martenstic transformation at room and low temperature, which mostly depend on microstructural aspects, influence the drawability of the materials. The drawability of the 304 ASS is very much steady when compared to the 316 ASS. In balance biaxial test, there is a decreased strain hardening rate due to the increase of the volume fraction of the induced martensite when compared to the uniaxial test[5].The ASS 304 material is very much suitable structural element at elevated temperatures and in nuclear reactors the temperature is very high therefore its tensile properties at elevated temperatures needs to be analysed with the knowledge of constitutive modes among which ANN is famous for its simplicity and accuracy.

The trained ANN model gives an excellent correlation coefficient and absolute average error values which represents a good accuracy of the model. The Artificial Neural Network (ANN) to predict the mechanical properties of AZ61 Mg alloy fabricated by equal channel angular pressing (ECAP)[6]. A back-propagation (BP) algorithm is used to train the neural network prediction models. Grain size, yield strength, and tensile strength of the alloy are predicted based on the number of ECAP passes[7]. The ANN predictions are shown to be in excellent agreement with experimental results, and the prediction error is shown to be minimal. These models can also be extended in the future to predict other properties, and possibly characterize other alloys.

Genetic Algorithm (GA) is a search algorithm based on the mechanics of natural selection and genetics and they combine survival of the fittest among string structures to form a search algorithm[8]. GA is particularly suitable for multi-parameter optimization problems with an objective function subject to numerous hard and soft constraints. The main idea of GA is to start with a population of solutions to a problem, and attempt to produce new generations of solutions which are better than the previous ones. GA operates through a simple cycle consisting of the following four stages: initialization, selection, crossover, and mutation. Fig.1. shows the basic steps of the basic genetic algorithm model[9].

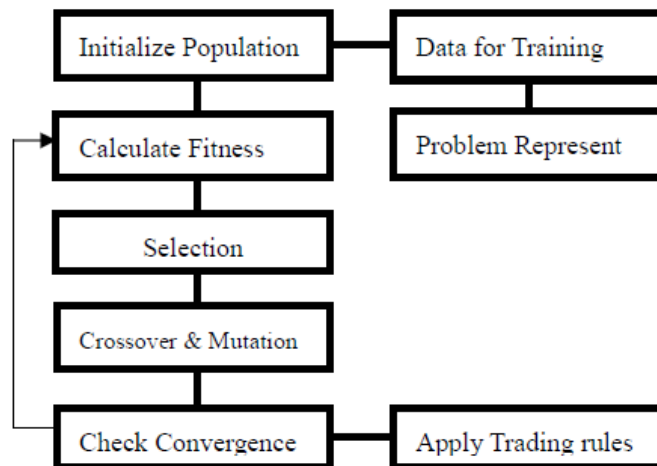


Fig.1. Basic Steps of the GA Model

Genetic algorithms are proven, theoretically and empirically, to provide a robust search in complex spaces, thereby offering a valid approach to problems requiring efficient and effective searches. To execute a particular optimization task using GA, it requires to address a genetic representation of candidate solutions, a way to create an initial population of solutions, an evaluation function which describes the quality of each individual, genetic operators that generate new variants during reproduction, and values for the parameters of the GA, such as population size, number of generations and probabilities of applying genetic operators.

In the initialization stage, a population of genetic structures (called chromosomes) that are randomly distributed in the solution space is selected as the starting point of the search. These chromosomes can be encoded using a variety of schemes including binary strings, real numbers or rules. After the initialization stage, each chromosome is evaluated using a user-defined fitness function. The goal of the fitness function is to numerically encode the performance of the chromosome. For real- world applications of optimization methods such as GA, the choice of the fitness function is the most critical step. The mean squarederror (MSE), which is the error between the desired and the predicted outputs as given by the equation (1)[10], is considered as the fitness function in the genetic algorithm.

$$MSE = \frac{1}{N} \sum_{i=1}^{patterns\ number} (y_i^{desired\ output} - y_i^{predicted\ output})^2 \quad (1)$$

In the present study, ANN-GA model is initially trained with one input neuron, representing the temperature and six output neurons, corresponding to the mechanical properties and twenty hidden neurons. The model has been trained with the desired value of MSE using the genetic algorithm for predicted the desired value of the output values.

2. Implementation

2.1. Experimentation on UTM Machine:

In this work, the material tested was Austenitic Stainless Steel 304 (ASS-304). In the previous study of author [“Study the Effect of Temperature on the Properties of ASS-304 Using ANN”, 23rd International Conference on Processing and Fabrication of Advanced Materials, 1186-1192, Dec 2014, IIT Roorkee], the specimens of ASS-304 steels were tested on a 5 ton UTM machine (Fig.2.) to calculate the material properties like Ultimate Tensile Strength (UTS), Yield Strength (YS), % Elongation, Strength Coefficient (K) and Work Hardening Exponent (n). The experiments were conducted from temperature 50⁰C to 650⁰C in the interval of 50⁰C. It was found out that as the temperature increases, there is a decrease in the values of YS, UTS, K and n values. But at 350⁰C these values starts increasing again due to blue brittle phenomenon which occurs due to impurities of Cr, Ni and other impurity materials. After 450⁰C these properties again starts decreasing due to material being in the plastic region.

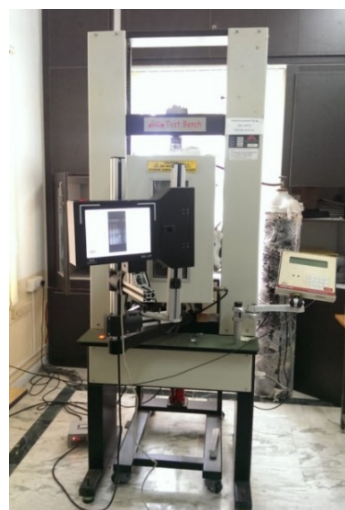


Fig.2. Universal Testing Machine

2.2. Development of ANN- GA Model:

The experimental data (Table 1.) was trained using Artificial Neural Network (ANN) model at unknown temperature with Back Propagation (BP) algorithm. 13 samples of input data i.e. temperature and 13 samples of 6 target data i.e. n, K, UTS, YS, Youngs, %elon were taken to train the network. This training stops when the validation error increased for six iterations, which occurred at 6th iteration. The performance plot which shows the training errors, validation errors and testing errors is shown in Fig.3. The network response is very promising; hence a new input of unknown temperature can be given to the network to predict the properties of the material as the outputs.

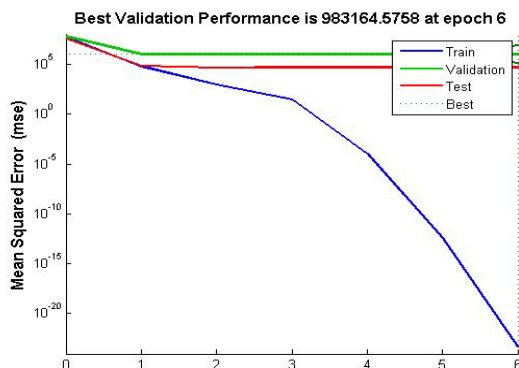


Fig.3. Performance plot

Table 1. Trained data Set

Temperature	N	K	UTS	YS	Youngs	%elon
50 ⁰ C	0.3706	1085.925	675	275.36	20652	58.3531
100 ⁰ C	0.3394	1029.912	636.6667	299.404	17612	56.93569
150 ⁰ C	0.3629	1032.048	578.3333	266.46	17764	42.52202
200 ⁰ C	0.3972	1000.691	516.6667	214.3147	20092	37.6805
250 ⁰ C	0.4184	1043.758	518.3333	225.72	15048	36.30065
300 ⁰ C	0.4474	1159.044	526.6667	221.2	13825	33.25284
350 ⁰ C	0.4932	1204.759	520	215.3503	10591	32.8554
400 ⁰ C	0.4119	1056.331	471.6667	231.3373	15773	36.96493
450 ⁰ C	0.3797	950.3859	500	203.895	22655	32.07232
500 ⁰ C	0.3751	848.985	458.3333	193.336	13182	34.00373
550 ⁰ C	0.3957	887.9735	440	195.0643	14273	33.90331
600 ⁰ C	0.3862	855.6576	395	184.31	15360	37.59177
650 ⁰ C	0.3942	675.6161	320	156.144	13012	30.86086

The BP algorithm employed in the training of the neural network derived from the gradient method requires an objective function which is continuously differentiable[11]. This might cause some problems in the learning process, such as the slow convergence, oscillation effect etc., which are due to the random selection of weight and threshold values. Hence, the genetic algorithm is used to optimize the artificial neural network by minimizing the mean squared error which is considered as the fitness function. A function can be written to accept the network, weights and biases, inputs and targets. This function may return the mean squared error based on the outputs and the targets as GA requires a function handle that only returns a scalar value. A basic BP neural network model is created with the definition of a MSE function handle to be passed to GA.

3. Results and Discussion

The concrete steps in implementing the ANN-GA algorithm are as follows:

- (i) Create the neural network model.
- (ii) Initialize the population.
- (iii) Compute the fitness value, MSE of the present population MSE can be considered as the count of fitness value.
- (iv) Chromosomes are generated. The encoded chromosomes are searched to minimize the fitness function.

In this phase, GA operates the process of crossover and mutation on initial chromosomes and iterates until the stopping conditions are satisfied. The population size is set to 20 organisms and the crossover and mutation rates are varied to prevent ANN from falling into a local minimum. The range of the crossover rate is set to 0.8 while the mutation rate ranges from 0.05 to 0.1. As the stopping condition, only 50 trials are permitted. The performance plots of the ANN-GA algorithm are shown in Fig.4. and Fig.5.

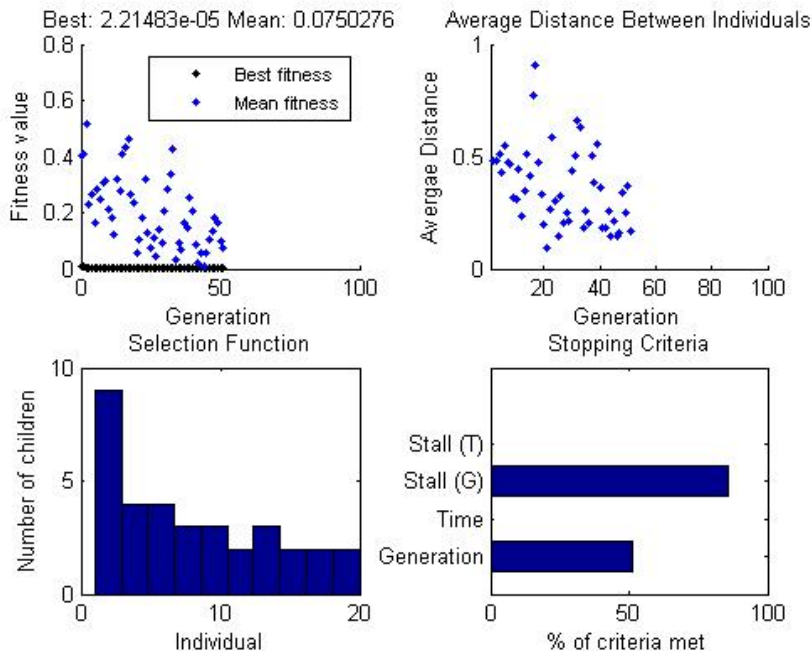


Fig. 4. Performance Plots of the Fitness, Distance, Selection and Stopping

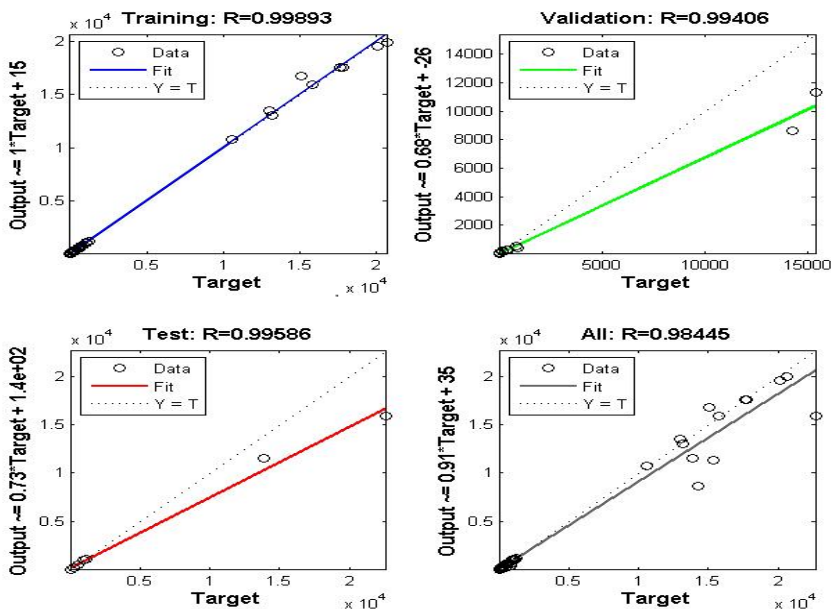


Fig.5. Performance Plots of the ANN-GA Algorithm

The proposed ANN-GA model is tested for new values of the temperature for predicting the mechanical properties of the ASS-304. The test results show that the hybrid ANN-GA model is more accurate, fast and effective method for prediction applications.

4. Conclusions

In this work, the MSE values of the neural network model were minimized using GA. The accurate results show that the proposed ANN-GA model can be considered a robust tool for prediction applications and is an effective mathematical model for assessing the mechanical properties of ASS-304 at elevated temperatures. The hybrid ANN-GA model is validated based on the statistical parameters like the mean square error and the convergence speed. The simulation results show that ANN-GA model gets great improvement in generalization ability, and has higher reliability in prediction when compared to ANN models. The results also show that genetic algorithm can be very good at speeding up convergence speed and solving the problem of local minimum to realize the global search.

5. Acknowledgment:

The financial support received for this research work from University Grants Commission, Government of India, MRP-4587/14 (SERO/UGC) is gratefully acknowledged.

References

- [1] A. K. Gupta, H. N. Krishnamurthy, Y. Singh, K. M. Prasad, and S. K. Singh, "Development of constitutive models for dynamic strain aging regime in Austenitic stainless steel 304," *Mater. Des.*, vol. 45, pp. 616–627, 2013.
- [2] X. Y. Wang and D. Y. Li, "Mechanical, electrochemical and tribological properties of nano-crystalline surface of 304 stainless steel," vol. 255, pp. 836–845, 2003.
- [3] M. Kaur, H. Singh, and S. Prakash, "A survey of the literature on the use of high velocity oxy-fuel spray technology for high temperature corrosion and erosion-corrosion resistant coatings," *Anti-Corrosion Methods Mater.*, vol. 55, no. 2, pp. 86–96, 2008.
- [4] M. Fujiwara, K. Yamazaki, M. Okamoto, J. Todoroki, T. Amano, T. Watanabe, T. Hayashi, H. Sanuki, N. Nakajima, and K. Itoh, "Large helical device (LHD) program," *J. fusion energy*, vol. 15, no. 1–2, pp. 7–153, 1996.
- [5] Z. Tourki, H. Bargui, and H. Sidhom, "The kinetic of induced martensitic formation and its effect on forming limit curves in the AISI 304 stainless steel," vol. 166, pp. 330–336, 2005.
- [6] L. Singaram, "Ann prediction models for mechanical properties of AZ 61 mg alloy fabricated by equal channel angular pressing," *Int. J. Res. Rev. Appl. Sci.*, vol. 8, no. 3, 2011.
- [7] F. Djavanroodi, B. Omranpour, and M. Sedighi, "Artificial neural network modeling of ECAP process," *Mater. Manuf. Process.*, vol. 28, no. 3, pp. 276–281, 2013.
- [8] L. D. Davis and M. Mitchell, "Handbook of Genetic Algorithms," pp. 1–6, 1991.
- [9] R. Naik, D. Ramesh, B. Manjula, and A. Govardhan, "Prediction of Stock Market Index Using Genetic Algorithm," *Comput. Eng. ...*, vol. 3, no. 7, pp. 162–172, 2012.
- [10] M. A. Mohandes, T. O. Halawani, S. Rehman, and A. A. Hussain, "Support vector machines for wind speed prediction," *Renew. Energy*, vol. 29, no. 6, pp. 939–947, 2004.
- [11] V. G. Gudise and G. K. Venayagamoorthy, "Comparison of particle swarm optimization and backpropagation as training algorithms for neural networks," in *Swarm Intelligence Symposium, 2003. SIS'03. Proceedings of the 2003 IEEE*, 2003, pp. 110–117.



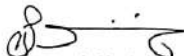
1st National Conference on
CONVERGENCE OF EMERGING TECHNOLOGIES IN COMPUTER SCIENCE & ENGINEERING
CETCSE-2K17

29th & 30th December, 2017, Hyderabad, Telangana.

Certificate of Presentation

This is to certify that Mr./Ms./Dr. V. padmakan
of VCBT visvesvaraya college of Engg & Tech, Hyd
has presented a Research Paper Titled Empirical Analysis of Software
Security Engineering - Phase wise
in the First National Conference on Convergence of Emerging Technologies in Computer Science & Engineering
organized by Department of Computer Science & Engineering, Nalla Narasimha Reddy Education Society's
Group of Institutions.


Convenor
CETCSE-2K17


General Chair
CETCSE-2K17





FC and ZFC magnetic properties of ferro-spinels (MFe_2O_4) prepared by solution-combustion method

G. Aravind, R. Vijaya Kumar, V. Nathaniyal, T. Rambabu, and D. Ravinder

Citation: [AIP Conference Proceedings](#) **1859**, 020079 (2017); doi: 10.1063/1.4990232

View online: <http://dx.doi.org/10.1063/1.4990232>

View Table of Contents: <http://aip.scitation.org/toc/apc/1859/1>

Published by the [American Institute of Physics](#)

FC and ZFC Magnetic Properties of Ferro-spinels (MFe_2O_4) Prepared by Solution-Combustion Method

G. Aravind ^{1,2,a}, R. Vijaya Kumar ³, V. Nathaniyal ¹, T. Rambabu ¹, D. Ravinder ¹

¹ Department of Physics, Osmania University, Hyderabad-500 007.

² Methodist College of Engineering & Technology, Hyderabad-500 001.

³ School of Physics, University of Hyderabad, Hyderabad-India.

^aCorresponding author: gunthaaravind@gmail.com

Abstract. Magnetic ferro-spinels MFe_2O_4 ($M=$ Co and Ni) prepared by citrate-gel solution combustion method using metal nitrates with low sintering temperature (500°C). From the XRD and TEM studies confirm that a nano crystalline nature of the prepared samples. Field Cooled (FC) and Zero Field Cooled (ZFC) magnetic studies of the prepared ferro-spinels are measured by using vibrating sample magnetometer (VSM). The resultant magnetization of the prepared samples as a function of an applied magnetic field 10 T was measured at two different temperatures 5 K and 310 K. Field Cooled (FC) and Zero Field Cooled (ZFC) magnetization measurements under an applied field of 100 Oe and 1000 Oe in the temperature range of 5–375 K were carried out, which shows the blocking temperature of these two samples at around 350 K.

Key words Spinel ferrites, citrate gel method, XRD, TEM, FC & ZFC

1. Introduction:

The expansion of the novel nano crystalline magnetic materials and their tunable electromagnetic properties has turned into one of the most important research goals of the 21st century. Ferri magnetic materials (ferrites) composed of iron oxides and metal oxides are more and tremendous magnetic materials broadly used in high frequency microwave applications like isolators, circulators, gyrators, phase shifters and cathode material in lithium ion batteries [1]. They exhibit both high electrical resistivity and useful magnetic properties which are not found in any other magnetic materials. In addition to their combined properties, they have very high degree of compositional variability. The crystal structure of ferrites is such that it can accommodate different cations at available sites with dissimilar valence states. Ferrites are distinct class of magnetic materials having spinel structure. They consist of abrupt magnetized domains and show the phenomenon of magnetic hysteresis and saturation magnetization. These ferrites have gained lot of interest because of their high electrical resistivity, low loss behavior and remarkably high electromagnetic flux induction.

The research on spinel ferrites is very mature, because of their potential applications and fascinating physics involved in it, even after so many decades, researchers are still interested in the design of various types of spinel ferrite materials, doped with different metallic ions with various valence states, synthesized by novel methods. It was observed that the air sintered spinel ferrites are characterized by microstructure consisting of relatively highly conductive grains separated by highly non conducting grain boundaries [2-3].

Nano crystalline $CoFe_2O_4$ is a well-known medium hard magnetic material, which has been analyzed due to its moderate coercivity, high chemical stability, fine electrical insulation, significant mechanical hardness and moderate saturation magnetization at room temperature. Due to their strong ferromagnetism and high Curie temperature cobalt ferrite is used in electronic appliances as it causes the materials to stay magnetized even when the applied magnetic field is turned off, leading to a useful way of storing information. It finds innumerable applications in stress sensors as precursors for making ferro fluids and also as magnetic refrigerants [4-5]. Nano crystalline $NiFe_2O_4$ is a soft ferri magnetic material due to its nano crystalline nature and useful properties, the material shows a good potential for novel applications in humidity, gas sensing [6] and drug delivery [7-8]. There are number of other applications in heterogeneous catalysis [9-11], adsorption, sensors and magnetic technologies. Normally, ferrites become super-paramagnetic at room temperature for nano particles of less crystallite size [12-13]. Super-paramagnetic nature of ferrites finds applications in Biomedical field, Magnetic Resonance Imaging (MRI) [14], Targeted drug delivery [15], Hyperthermia for cancer treatment [16].

Solution -combustion method is characterized by the high temperature, fast heating rates and short reaction times. These characteristics make the solution-combustion method an attractive route for the manufacture of nano crystalline materials at lower costs compared with the conventional ceramic methods. Relatively simple equipment,

stabilization of metastable phases, formation of virtually any size and shape particles etc are the other advantages of the solution- combustion method.

All the facts revealed from the literature survey motivated us to prepare cobalt ferrite and nickel ferrites. In the present investigation we prepare the magnetic spinel ferrites MFe_2O_4 ($M= Co$ and Ni) by citrate-gel auto combustion method using nitrates of respective elements and by keeping 1:1 ratio of metal nitrates to citric acid with low sintering temperature ($500^\circ C$). The single phase of the prepared samples can be confirmed by the x-ray diffraction analysis and nano crystalline nature is observed from the transmission electron microscopy. Field Cooled (FC) and Zero Field Cooled (ZFC) magnetic studies of the samples can be measured by using vibrating sample magnetometer (VSM) which shows the super-paramagnetic nature of the prepared samples.

2. Experimental Techniques:

The nano crystalline spinel ferrites MFe_2O_4 ($M= Co$ and Ni) were prepared by citrate-nitrate auto combustion method and flow chat for preparation as shown in fig(1). The AR grade citric acid, cobalt nitrate, nickel nitrate, ferric nitrate and ammonia solution were used as raw materials. The products of the system were produced by keeping the metal nitrates to citric acid ratio 1:1. Reaction process was carried by air atmosphere without protection of inert gases.

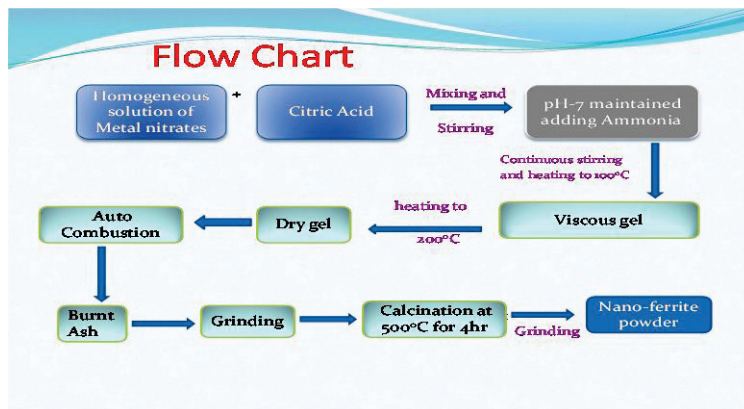


Fig (1) Flow chart for preparation

Required chemicals were weighed and dissolved separately in minimum quantity of distilled water. All the individual solutions were mixed together and then the ammonia solution was slowly added to adjust the pH value at 7. The proliferation of nitrate ions at low pH value is likely to decrease the enthalpy of exothermic reaction by decreasing the fuel to oxidizing ratio. Thus, the rate of combustion reaction decreases and particles agglomerates [17] so the pH value of the solution was maintained at 7, to avoid the agglomeration and preserve the stoichiometry of the mixed solution. The resultant solution was kept on a hot plate magnetic stirrer at $100^\circ C$ till gels were formed, after that, increasing the temperature up to $200^\circ C$, the gels self-ignited in an auto combustion manner till whole citrate complex was consumed to yield nano ferrite powders. These synthesized ferrite powders were annealed at $500^\circ C$ for 4 hours in a muffle furnace [18]. The heat treated powders were used for further characterization. The overall reaction for formation of nickel ferrite is given below.



From the above equations it is observed that the auto combustion synthesis process produces CO_2 , H_2O , and N_2 without the necessity of getting oxygen from outside

The phase confirmation of the synthesized samples was carried out by Philips X-ray diffractometer (Model 3710) using $Cu K_\alpha$ radiation of wavelength 1.5405 \AA at room temperature by continuous scanning in the range of Bragg's angles 10° to 80° in steps of $2^\circ/\text{min}$ to investigate the phase and crystalline size. The average crystalline size of the ferrites was determined from the measured width of their diffraction pattern using the Debye scherrer's formula

$$D = 0.91\lambda / \beta \cos\theta \quad (1)$$

Where λ is the wavelength of the X-ray used for diffraction, β is the full width half maximum (FWHM) in radians.

Transmission electron microscopy (TEM) measurements were recorded on Philips apparatus (CM 200 model). Field Cooled (FC) and Zero Field Cooled (ZFC) magnetic studies of the samples can be measured by using vibrating sample magnetometer (VSM Lakeshore, model 7307).

3. Results and Discussion:

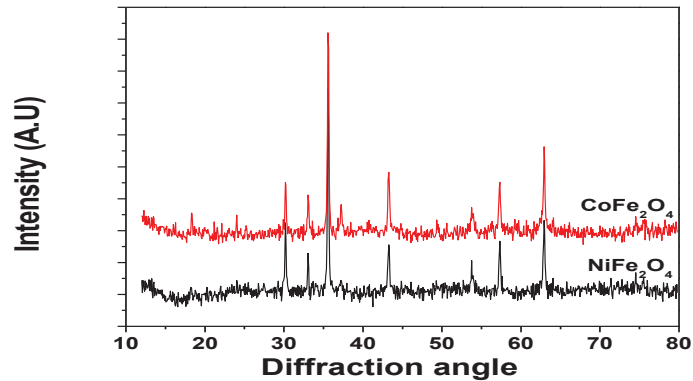
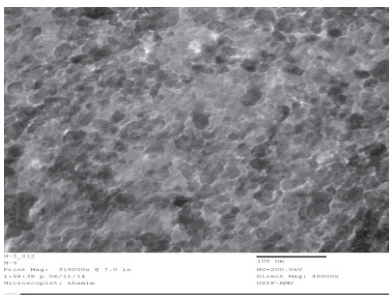
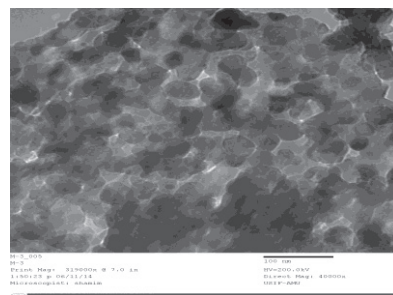


Figure (2) XRD Pattern of prepared nano ferrites

XRD pattern of the prepared samples were shown in below fig (1) and confirmed the single phase spinel structure which indicates the solubility of cations into their relevant lattice sites. The positions of the reflection peaks for investigated samples are almost identical to the corresponding peaks for the bulk material, this implies that the basic structure of the nano crystalline materials is basically same like the bulk counterparts. The peak broadening in the XRD pattern of the investigated samples confirmed the formation of nano-size crystallites. All main diffraction planes are indexed as (220), (311), (400), (422), (511) and (440) with maximum diffraction intensity from (311) plane co-inside with the standard pattern reported by the Joint Committee on Powder Diffraction Standards (JCPDS) for single phase cubic spinel with file no: 00-013-0207 with space group $Fd\bar{3}m$. No characteristic peaks of impurities are detected in the XRD pattern. The crystallite size of the samples was calculated by measuring the FWHM of the most intensive peak (311). The average crystallite size of the nickel ferrite is 43 nm and cobalt ferrite is 36 nm which is already published in our earlier paper [19-20].



(3a) TEM image of CoFe_2O_4



(3b) TEM image of NiFe_2O_4

Fig (3a & 3b) shows TEM micrographs of the prepared nano crystalline cobalt ferrites and nickel ferrites respectively. Uniform spherical agglomerated particles in both morphology and size were obtained. The particle agglomeration is due to the magnetic interaction between the particles and permanent magnetic moment experienced by the nano particles which is proportional to their volume [21-23]. The TEM estimated particle size of the samples are larger than the average crystallite size calculated from the X-ray diffraction analysis, which is explained by following two reasons: (1) In X-ray diffraction analysis, X-rays can notice only the grains and they cannot considered the disordered grain boundaries which occupy considerable volume; (2) there is a chance of the accumulation of more than one crystallite forming an agglomeration of particles [24-25].

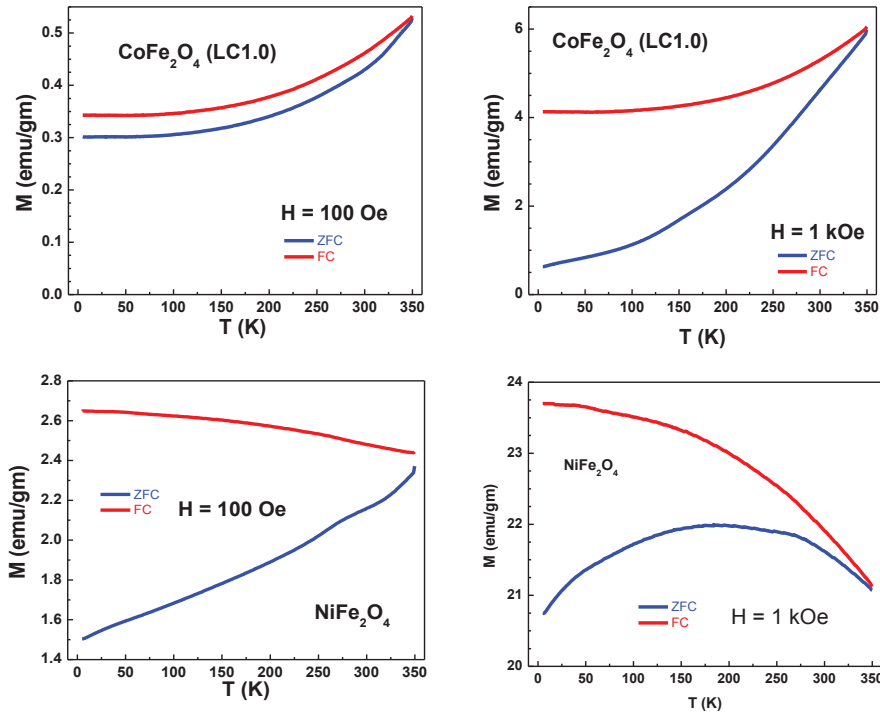


Fig (4) Magnetization-Temperature curves recorded in FC and ZFC modes for the sample CoFe_2O_4 and NiFe_2O_4 in an external magnetic field of 100 Oe and 1k Oe.

The magnetic behavior of investigated samples was analyzed from the temperature dependence of the magnetization measured in zero field cooled and field cooled modes which was shown in fig (4). In ZFC procedure, the sample is cooled (usually down to the liquid helium temperature) in the absence of a magnetic field and then a moderate measuring field is applied (here 100 Oe and 1000 Oe). Then the magnetization (M) values being recorded by gradually raising the temperature. The FC procedure differs from ZFC, only by the fact that the sample is cooled in a non-zero magnetic field. The discrepancy between the FC and ZFC magnetization is found in both the samples at different applied fields in the whole range of measured temperatures (5K to 375K) which indicates super-paramagnetic behavior [26].

The temperature at which this bifurcation in the two modes (FC & ZFC) is observed is defined as bifurcation temperature or blocking temperature (T_b). It is observed that the blocking temperature did not change with the increase in applied field but shows a strong bifurcation in the FC and ZFC curves under higher applied field i.e. at 1 k Oe, showing irreversibility of FC and ZFC magnetization curves. For both the samples the bifurcation or blocking temperature is observed at around 350 K, below blocking temperature the material shows some hysteresis and hence behaves as ferromagnetic material and above blocking temperature, hysteresis disappears and the material behaves as super-paramagnetic.

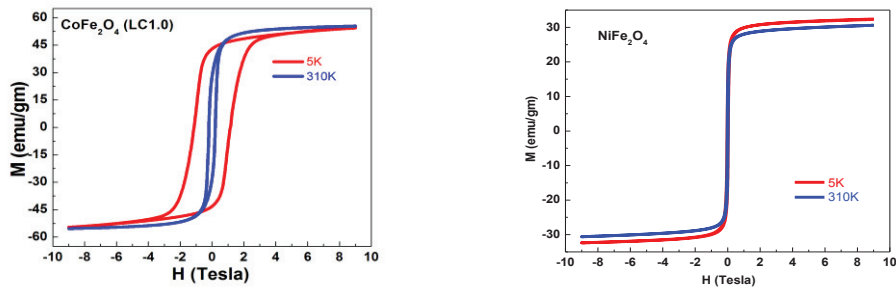


Fig (5) Hysteresis Curves for CoFe_2O_4 and NiFe_2O_4 at 5K and 310K

Table1. Coercivity (H_c) and Remanence (M_r) values of cobalt ferrite and nickel ferrites

Magnetic parameters	NiFe ₂ O ₄		CoFe ₂ O ₄	
	5K	310K	5K	310K
Coercivity(H_c) Tesla	0.04	0.02	1.09	0.19
Remanence (M_r) (emu/gm)	16.65	14.59	43.30	30.99

Fig 5. shows Magnetization Hysteresis curves for NiFe₂O₄ and CoFe₂O₄ samples at 5 K and 310 K. It is observed that the coercivity is more at lower temperature and it decreases with increase in temperature. The values of Coercivity (H_c) and remanence (M_r) were measured from the hysteresis curves and were recorded in table 1.

Acknowledgements

One of the authors Dr. V. Nathaniel is very thankful to UGC-Delhi for awarding Minor Research Project. One of the authors Dr. G.Aravind is very thankful to Prof. M. Lakshmipathi Rao, Principal, Methodist College of Engineering and Technology.

References

1. Rajesh Cheraku, G. Govindaraj, Lakshmi Vijayan, Materials Chemistry and Physics, (2014) 1-4.
2. Khalid Mujasam Batoo, Shalendra Kumar, Chan Gyu Lee, Alimuddin, *Current Applied Physics* 9 (2009) 1072-1078.
3. Sangeeta Thakur, S.C. Katyal, A.Gupta, V.R.Reddy, S.K.Sharma, M.Knobel, M.Singh, *J.Phys.Chem. C* 2009, 113, 20785-20794.
4. S. Kiickelhaus, A. C Tedesco, D. M Oliveira. P. C. Morais, G. R. Boaventura, Z. G. M. Lacava., *J. App. Physics* 97 (2005) 10Q910.
5. Srikanth Hariharan, James Gass. *Rev. Adv. Mater. Sci.* 10 (2005) 398.
6. Shimizu. Y., Arai. H., Seiyama. T., *Sens. Actuators* 7 (1985) 11.
7. Chen. N.S., Yang. X.J., Liu. E.S., Huang. J.L., *Sens. Actuators B* 66 (2000) 178.
8. Goldmann. A., *Modern Ferrite Technology*, Van Nostrand Reinhold, New York (1990)71
9. Coquay. P., Peigney. A., De Grave. E., Vandenbergh. R.E., Laurent. C., *J. Phys Chem.B* 106 (2002) 13199.
10. Astorino. E., Busca. G., Ramis. G., Willey. R., *J. Catal. Lett.* 23 (1994) 353.
11. Busca. G., Finocchio. E., Lorenzelli. V., Trombetta. M., Rossini. S.A., *J. Chem. Soc. Faraday Trans.* 92 (1996) 4687.
12. Joong-Hee Nam, Won Ki Kim Sang Jin Park, *Phys. Status Solidi (a)* 201 (2004) 1838.
13. Chao Liu" Z John Zhang, *Chemistry of Materials* 13 (2001) 2092.
14. Y.W. Jun, Y.M. Huh, J.S. Choi, J.H. Lee, H.T. Song, S. Kim, S. Yoon, K.S. Kim, J.S. Suh, *J. Cheon. J. Am. Chem. Soc.* 127(2005)5732
15. A. Ito, Y. Kuga, H. Honda, H. Kikkawa, A. Horiuchi, Y. Watanabe and T. Kobayash, *Cancer Let.* 212(2004)167
16. R. Ivkov, S.J. Denardo, W. Daum, A.R. Foreman, R.C. Goldstein, V.S. Nemkov and G.L. Denardo, *Clin. Cancer Res.* 11(2005) 7093
- 17.L.C.Pathak,T.B.Singh,A.K.Das,S.Verma,P.Ramachanderrao,*mater Letters*57(2002)380-385.
18. J.Chandra das,M.Balasubramanian,K.H.Kim,*Mater Manuf process*25 (2010)1449-1453
19. G.Aravind, D.Ravinder,V.Nathaniel, *Advanced Material Letters-VBRI Press-* 2015, 6(2), 179-185,
20. Structural and Electrical Properties of Li-Ni nano ferrites Synthesized by citrate gel auto combustion method, G.Aravind, D.Ravinder, V.Nathaniel, *Physics Research International*, Vol 2014, Article ID 672739,11
21. M.A. Gabal, Y.M. Al Angari, F.A. Al-Agel, *J of Molecular Structure* 1035 (2013) 341-347.
22. S.T. Alone, Sagar E.Shirasath, R.H. Kadem, K.M.Jadhav, *J of Alloys and Compounds* 509 (2011) 5055.
23. M.A.Gabal, R.M. El-Shistawy, Y.M. Al Angari, *J of Magn and Magn Matr* 324 (2012). 2258.
24. M.K. El Nimr, B.M. Moharram, S.A. Saafan, S.T. Assar, *J of Magn and Magn Mater* 322 (2010) 2108-2112.
25. S.A. Saafan, S.T. Assar, B.M. Moharram, M.K. El Nimr, 322 (2010) 628-632.
26. Natasa Jovic, Bratislav Antic, Gerado F.Goya, and Vojislav Spasojevic, *Current nano Science*, 2012, 000-000.

Single Lead EEG Acquisition System For Health Care Applications

Bhavana Gaddipati
Dept. of ECE, Vignan's University
Guntur, AP, INDIA
bhavana.uv132@gmail.com

Usha Rani Nelakuditi
Dept. of ECE, Vignan's University
Guntur, AP, INDIA
usharani.nsai@gmail.com

John William Carey Medithe
Dept. of ECE, Vignan's University
Guntur, AP, INDIA
careymedithe@gmail.com

Abstract—It is very much difficult to call the patient every time to have EEG test, when a physician wants to examine the outcome of the diagnosis. Currently, there are many data acquisition schemes for monitoring the signals from the psyche and designed to perform EEG in the Recording Room. But, this system extends a design of portable circuitry for rapid and convenient use in health care. High gain precision instrumentation amplifier is designed in hardware and that the output is connected to the analog input of NI myDAQ which is interfaced via USB to computer. Filters are coded in NI Labview and applied to the signal to have smooth analysis. This system can amplify signals more and better noise eliminating options compared to other commercial EEG data acquisition systems. Portable Single lead EEG system is very much used to observe patients suffering from brain damage or any injuries in the brain at home or in the conveyance.

Keywords—Acquisition, EEG, Electrodes, Filters, NI myDAQ.

I. INTRODUCTION

Electroencephalography (EEG) is a test used for monitoring and measuring the different electrical activities of the brain. Brain consists of millions of neurons. The discharges of neurons induces different amount of potential over the scalp for different states of subjects alertness, external stimuli and so on. This brain electrical activity is acquired using electrodes which are placed over the scalp. These electric discharges would be in the order of microvolts. It can be acquired in the order of millivolts when recording is taken using subdural electrodes. As EEG bio potentials are in the order of microvolts are very much prone to get contaminated with other bio potentials like artifacts and noise. Although, approximately 0.5 to 30 Hz of frequency range are considered in clinical interest to treat various brain disorders. Long time tendency to occurrence of seizures in particular region may result in brain disorder like Epilepsy and Grandmal etc.

A. EEG Frequencies:

Along with the position of the electrode the brain frequencies are changed so EEG waveforms are classified into five sets (alpha, beta, theta, and delta) [1, 2, 5]. The characteristics of different frequencies and their state of occurrence, outcomes and their abnormalities are classified below.

- Alpha waves
 - Occur in the frequency range of 8 and 13 Hz.

- Region: Alpha waves are observed better in posterior and occipital regions.
- Outcome of this frequency: Alpha waves are found in normal person when they are relaxed and resting position. These waves can disappear when we can open the eyes or alert position where there attention is directed to specific work.
- Abnormality: If present in frontal regions may suspect as depression and attention problems.
- Beta waves
 - Occur in the frequency range of 13-30 Hz, sometimes it can extend to 50Hz.
 - Region: These frequency range found in parietal and frontal region of the scalp.
 - Outcome of this frequency: Beta wave activities are present when the person is in tension and intense mental activity with their eyes open.
 - Abnormality: Deficient beta may rise to lack of concentration and problem solving.
- Theta waves
 - Occur in the frequency range of 4 to 8 Hz with large amplitude.
 - Region: These mainly occur in the parietal and temporal regions.
 - Outcome of this frequency: Theta waves are abnormal in small children when awake and adults during sleep.
 - Abnormality: If seen in awake adults
- Delta waves
 - Occur in the frequency range of 0.5 to 4 Hz with high amplitude.
 - Region: They occur within the cortex and also they are found in central cerebrum, mostly parietal lobes.
 - Outcome of this frequency: Delta is normal in infants and occurs during sleep in adults.
 - Abnormality: If seen in awake adults.
- Gamma waves
 - Occur in the frequency range of 36-44 Hz.

- Region: In general the slowest cortical rhythms is related to an ideal brain that occur in a location of cortex.
- Outcome of this frequency: During short-term memory matching for recognized sounds, objects and other sensations.
- Abnormality: when for continuous for a long time

The graphical representation EEG frequencies are shown below Fig.1.

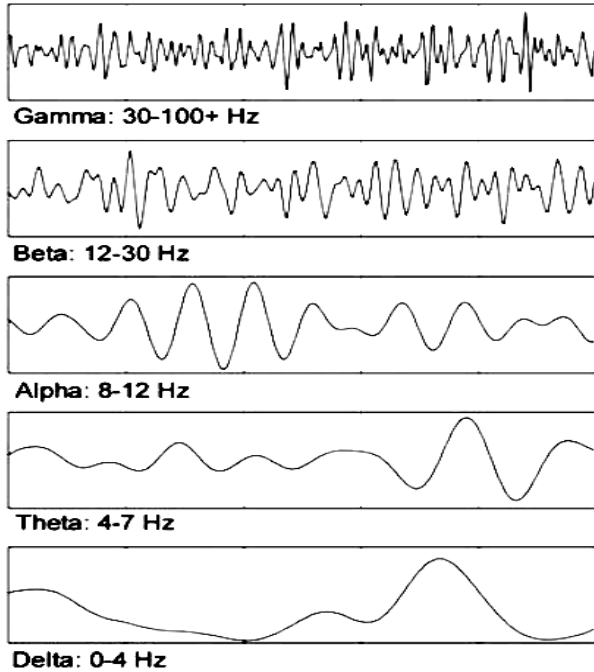


Fig. 1. Graphical representation of EEG Frequencies.

B. EEG Health Applications:

EEG can be used to monitor and diagnose different Neuro parameters. The major health applications is shown below but not limited [2, 3].

- To monitor cognitive engagement (alpha rhythm).
- To monitor alertness, coma and brain death.
- To analyse brain development.
- Locate areas of damage following head injury, stroke, tumour, etc.
- Investigate sleep disorder and physiology.

II. SYSTEM CONSTRUCTION

To acquire the EEG signal and to have better examination and analysis, International Federation of Clinical Neurophysiology (IFCN) suggested a standard for secure acquisition of EEG for clinical practices. The American Clinical Neurophysiology Society has suggested the usage of a minimum of 21 electrodes in acquisition system called International 10-20 [1]. This standard gives location and

naming of electrodes placed over the scalp. The electrodes placed on the left hemisphere of the scalp are named in odd numbers, while the right hemisphere named with even numbers. Differential gain of the two neighboring electrodes forms a channel called bipolar montage. It can be called as referential montage when acquisition with a common reference. Electrodes which are positioned over the scalp act as a transducer gives the resulting output as a voltage over a period of time. Midline electrodes are marked as Z while, other points marked as Front polar (Fp), central (c), Parietal (P), Occipital (O) and Temporal (T).

The single lead EEG acquisition system is constructed to have simple and low noise acquisition. This consists of a high gain instrumentation amplifier followed by on-screen filtering, which is coded in NI Labview. The flow diagram of the acquisition process is shown below Fig. 2.

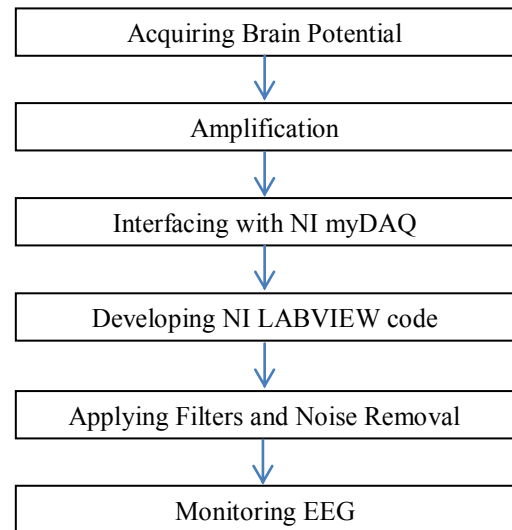


Fig. 2. Flow diagram of EEG Acquisition system design.

The single lead EEG system is very much used to monitor while mobile treatment and it is greatly helpful in study of particular brain disorder at particular region. The stages of development of single lead EEG system using NI myDAQ are described.

This single lead EEG acquisition system is designed to specific target group who is unable and not willing to have the conventional complex EEG test at medical centre. This system can also have the possibility to the physician to monitor patient EEG remotely.

A. Amplification and Filtering

Amplification of the bio-potential plays vital role in EEG acquisition process. Because the brain signal obtained over the scalp has potential in order of micro volts, which is very much difficult for the physician to analyze and interpret.

Instrumentation amplifier has excellent accuracy and high common mode rejection ratio (CMMR) has very low offset voltage of 50uv and low drift voltage. High CMMR can able to amplify low difference signals [5, 8]. Instrumentation amplifier

consists of two different stages. First stage consists of high impedance for both input terminals and gain will be fixed with adjusting resistor value R_G . In the second stage, it consists of differential amplifier which varies in polarity and amplitude. Thus, it gives high performance and precision in acquiring EEG signal. The overall gain of the instrumentation amplifier depends on adjusting R_G , where it is inversely proportional to output gain. The schematic diagram of the instrumentation amplifier is shown below in Fig. 3.

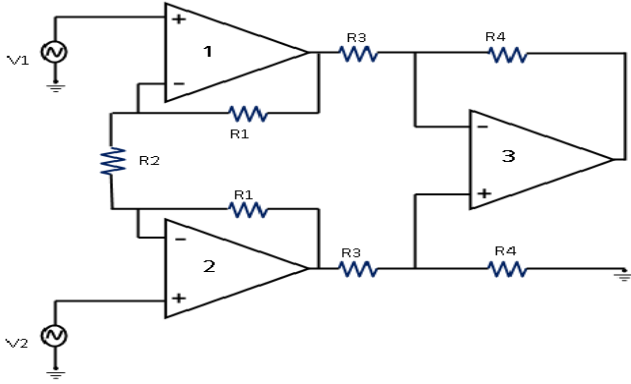


Fig. 3. Schematic diagram of Instrumentation Amplifier.

Gain of the amplifier is given as

$$V_0 = (V_2 - V_1) \frac{R_4}{R_3} \left[1 + \frac{2R_1}{R_2} \right] \quad (1)$$

Therefore the differential gain G is

$$G = \frac{R_4}{R_3} \left[1 + \frac{2R_1}{R_2} \right] \quad (2)$$

B. Filtering:

Although EEG signals are very weak so that they can easily contaminate with noise and other artifacts. Therefore, it is necessary to improve the signal by applying filters. All filters applied on to the analog output of the instrumentation amplifier are coded in Lab view. As 0.5 to 33 Hz of frequency is considered in clinical applications, band pass filter is used to reject a different frequency which does not match with clinical range. The filtered output can be monitored in the waveform chart located on the front panel.

C. Interfacing with NI myDAQ

NI myDAQ is a data acquisition system which contains Analog Input (contains 2 channels with 16 bits), Analog Output (also contains 2 channels with 16 bits and also contain 3.5 mm stereo jack), Digital I/O (8 DIO lines), counters (counter, timer), Integrated DMM (V, A, Ohm) and power supply (+/- 15 V) [11].

Data acquisition is the process of measuring the electrical potential or physical process such as current, voltage, temperature, etc. Data acquisition can be done with different types of sensors. NI myDAQ is the hardware that connects the analog output of the amplifier to the computer via USB. In this scenario, the analog output of the instrumentation amplifier is

connected to the analog input of the NI myDAQ i.e., A0. Where myDAQ is interfaced and powered via USB to computer.

D. Developing Labview Code

The code is developed in NI Labview, using DAQ assistant in the measurement I/O palette in the rear panel. Here, the required analog input slot has to be selected as A0. The resultant output can be monitored in the waveform chart of the front panel. Entire Labview code is placed in while loop to have continuous acquisition. The code developed in NI Labview for acquisition of EEG is shown in Fig. 4.

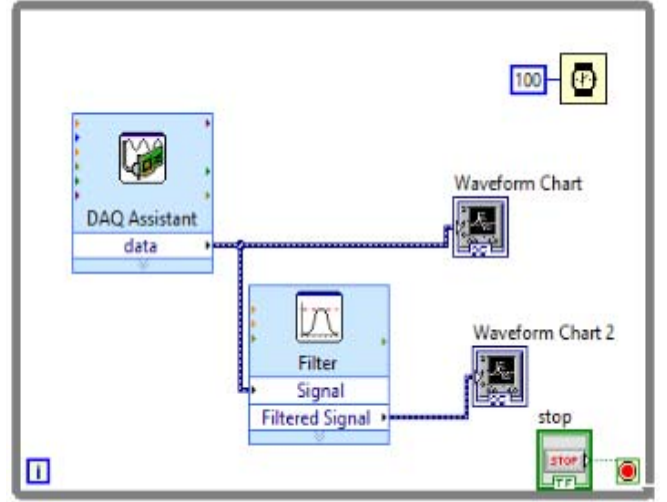
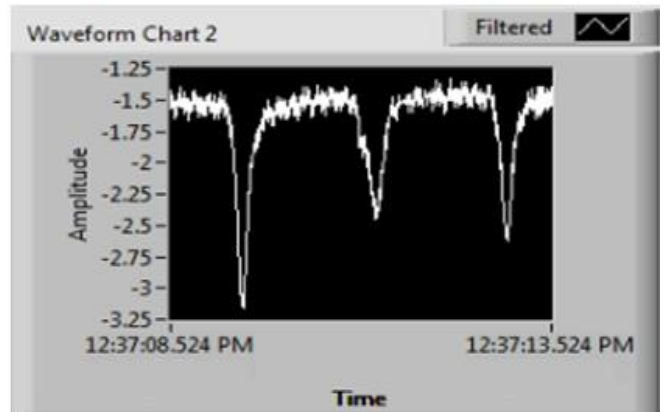


Fig. 4. myDAQ using Lab View.

III. RESULTS

After developing the circuitry and interfacing with NI myDAQ. The data is processed in NI Labview development software. The electrode is placed on the forehead and reference electrode on the left ear of the participant. Now, the participants were asked to blink an eye. Using this system the blink artifact in EEG signal can be monitored efficiently. The contamination of Blink artifact into the frontal region of EEG is displayed in the waveform chart, which is shown in below Fig. 5.



Scale: X-axis Time (s), Y-axis Amplitude (v/div)

Fig. 5. Blink acquisition in frontal region.

IV. CONCLUSION

A single lead EEG amplifier with active electrodes is designed and implemented using NI LABVIEW with interface of NI myDAQ. The Portable EEG acquisition is used to record the brain activity at a particular point or on specific lobe. It is very much useful to observe the seizures at a particular point on the psyche. Design is tested and verified on number of participants. The clear and precise acquisition depends on the filtering stages for the reduction of noise and to have better EEG signal.

V. ACKNOWLEDGEMENT

The authors would like to thank for the funding support from Department of Science and Technology (DST) as a grant SERC/ET-0153/2012 and Vignan University to carry out this work.

REFERENCES

- [1] Electroencephalography (EEG). [Online]. Available: <https://en.wikipedia.org/wiki/Electroencephalography>
- [2] Teplan, "Fundamentals of EEG Measurement," *Measurement Science Review*, vol. 2, sec. 2, 2002, pp. 1-11.
- [3] M. R. Croft and R. Barry, "Removal of ocular artifact from the EEG: a review," *Neurophysiologie Clinique/Clinical Neurophysiology*, vol. 30, iss. 1, Feb. 2000, pp. 5-19.
- [4] R. Homan, J. Herman and P. Purdy, "Cerebral location of international 10–20 system electrode placement," *Electroencephalography and Clinical Neurophysiology*, vol. 66, iss. 4, Apr. 1987, pp. 376-382.
- [5] Noor Ashraaf Noorazman and Nor Hidayati Aziz, "Portable EEG Signal Acquisition System," *College Science in India*, Feb. 2009, pp. 12-19.
- [6] D. Kim, K. Hong and K. Chung, "Implementation of portable multi-channel EEG and head motion signal acquisition system," in *Proc. of IEEE 8th International Conference on Computing and Networking Technology (ICCNT 2012)*, Gueongju, Aug. 2012, pp. 370-375.
- [7] The Experimental Portable EEG/EMG Amplifier, 2003. [Online]. Available: http://feihu.eng.ua.edu/WSN_EEG.pdf
- [8] L. Zhu, H. Chen, X. Zhang, K. Guo, S. Wang, Y. Wang, W. Pei and H. Chen, "Design of Portable Multi-Channel EEG Signal Acquisition System," in *Proc. of IEEE 2nd International Conference on Biomedical Engineering and Informatics*, Tianjin, Oct. 2009, pp. 1-4.
- [9] B. Luan, M. Sun and W. Jia, "Portable amplifier design for a novel EEG monitor in point-of-care applications," in *Proc. of IEEE 38th Annual Northeast Bioengineering Conference (NEBEC 2012)*, Philadelphia, PA, March 2012, pp. 388-389.
- [10] Amlan Jyoti Bhagawati and Riku Chutia, "Design of single channel portable eeg signal acquisition system for brain computer interface application," *International Journal of Biomedical Engineering and Science (IJBES 2016)*, vol. 3, iss. 1, Jan. 2016, pp. 37-44.
- [11] USER GUIDE AND SPECIFICATIONS NI MYDAQ. [Online]. Available: http://sukjaro.eu/ELFT-NI-palyazat/myDAQ_Manual.pdf
- [12] Z. Dan, Z. Xifeng and G. Qiangang, "An Identification System Based on Portable EEG Acquisition Equipment," in *Proc. of IEEE 3rd International Conference on Intelligent System Design and Engineering Applications (ISDEA 2013)*, Hong Kong, Jan. 2013, pp. 281-284.
- [13] B. Drakulic, S. Berry and M. Sterman, "A portable EEG recording system," in *Proc. of IEEE Twenty-First Century the Annual International Engineering in Medicine and Biology Society*, vol. 5, Seattle, WA, Nov. 1989, pp. 1395-1396.
- [14] EEG Frequencies. [Online]. Available: <http://neurosky.com/2015/05/greek-alphabet-soup-making-sense-of-eeg-bands/>
- [15] J. Medithe and U. Nelakuditi, "Removal of Ocular Artifacts in EEG," in *IEEE International Conference on Intelligent Systems and Control (ISCO-2016)*, Coimbatore, India, Jan. 2016.
- [16] J. Medithe and U. Nelakuditi, "Study of Normal and Abnormal EEG," in *IEEE International Conference on Advanced Computing and Communication Systems (ICACCS-2016)*, Coimbatore, India, Jan. 2016.

Institutional Sign In

Browse

My Settings

Get Help

Subscribe

Conferences > 2016 International Conference...

Back to Results

Performance comparison of various thresholding techniques on the removal of ocular artifacts in The EEG signals

Publisher: IEEE

<< Results

3 Author(s)

B. Krishna Kumar ; K.V.S.V.R. Prasad ; D. Alekhya [View All Authors](#)

124 Full Text Views

Export to

Collabratec

Alerts

Manage

Content Alerts

Add to Citation

Alerts

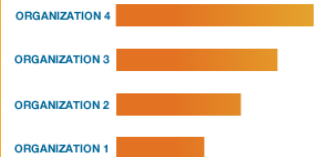
More Like This

Bessel k-form parameters in the dual tree complex wavelet transform domain for the detection of epilepsy and seizure
8th International Conference on Electrical and Computer Engineering
Published: 2014

Butterworth Bandpass and Stationary Wavelet Transform Filter Comparison for Electroencephalography Signal
2015 6th International Conference on Intelligent Systems, Modelling and Simulation
Published: 2015

[View More](#)

Top Organizations with Patents on Technologies Mentioned in This Article



Abstract

Document Sections

- I. Introduction
- II. Wavelet Transform
- III Methodology
- IV Conclusion

Authors

Figures

References

Keywords

Metrics

More Like This

Download PDF

Abstract: Electro-encephalogram (EEG) is the electrical activity of brain cell groups in the cerebral cortex or the scalp surface. It plays an important role in studying the patient... [View more](#)

Metadata

Abstract: Electro-encephalogram (EEG) is the electrical activity of brain cell groups in the cerebral cortex or the scalp surface. It plays an important role in studying the patient mental condition and Human Machine interfacing. Normal EEG signals can avail in the band of DC to 60 Hz frequencies with a few hundreds of micro volts of strength. Ocular artifacts and muscular noise with similar statistical properties are the major challenges which make the analysis more complex and may yields wrong interpretation. Here in this paper we discussed various thresholding techniques in the removal of ocular artifacts (OA) present in the EEG signal and there by compared performance these thresholding techniques in the removal of OA's with the help of various statistical parameters. In this paper the collected EEG signal is decomposed to 4 levels using db10 and sym8 wavelets and later threshold the detail coefficients using various thresholding techniques and estimated the statistical parameters of it.

Published in: 2016 International Conference on Inventive Computation Technologies (ICICT)

Date of Conference: 26-27 Aug. 2016 **INSPEC Accession Number:** 16620584

Date Added to IEEE Xplore: 26 January 2017 **DOI:** 10.1109/INVENTIVE.2016.7830179

Publisher: IEEE

ISBN Information:

Conference Location: Coimbatore, India

Contents

I. Introduction

Electrooculography (EOG) artifacts inevitably and frequently interfere

Electroencephalography (EEG) artifacts inevitably and frequently interfere with the electroencephalogram (EEG) signals. Eye-movement and eye-blink artifacts are the main sources of ocular artifacts. The frequency components of EEG signals are in the order of just a few up to 200 μV , and their frequency content differs among the different neurological rhythms, such as, alpha, beta, delta and theta rhythms [1]. However, artifacts and noise are the outstanding enemies of high quality EEG signals. Their presence is thus crucial for the accurate evaluation of EEG signal. They fall into two major categories: technical and physiological artifacts. The technical artifacts are often found in power line noise 50/60Hz results from poor electrode application on the scalp and transducer's artifacts. The physiological artifacts are often due to ocular, heart and muscular activity; are the EMG, EOG and ECG artifacts respectively [2].

Sign in to Continue Reading

Authors	▼
Figures	▼
References	▼
Keywords	▼
Metrics	▼

IEEE Account

Profile Information

Purchase Details

Need Help?

Other

A not-for-profit organization, IEEE is the world's largest technical professional organization dedicated to advancing technology for the benefit of humanity.
 © Copyright 2019 IEEE - All rights reserved. Use of this web site signifies your agreement to the terms and conditions.

US & Canada: +1 800 678 4333
 Worldwide: +1 732 981 0060

IEEE Account

- » Change Username/Password
- » Update Address

Purchase Details

- » Payment Options
- » Order History
- » View Purchased Documents

Profile Information

- » Communications Preferences
- » Profession and Education
- » Technical Interests

Need Help?

- » **US & Canada:** +1 800 678 4333
- » **Worldwide:** +1 732 981 0060
- » Contact & Support

[About IEEE Xplore](#) | [Contact Us](#) | [Help](#) | [Accessibility](#) | [Terms of Use](#) | [Nondiscrimination Policy](#) | [Sitemap](#) | [Privacy & Opting Out of Cookies](#)

A not-for-profit organization, IEEE is the world's largest technical professional organization dedicated to advancing technology for the benefit of humanity.
 © Copyright 2019 IEEE - All rights reserved. Use of this web site signifies your agreement to the terms and conditions.

Performance Comparison Of Various Thresholding Techniques On The Removal Of Ocular Artifacts In The EEG Signals

B.Krishna Kumar¹, Dr.K.V.S.V.R .Prasad² and D.Alekhy³

¹ Research Scholar, JNTU Hyderabad, TS, INDIA. E-mail : saisantu2004@yahoo.co.in

² Prof & Head Dept. of ECE, D.M.S.S.V.H Engg.College, Machilipatnam, AP, INDIA. E-mail: kvsvr@yahoo.com

³ IV B.Tech (ECE) student, JNTU Hyderabad, TS, INDIA. E-mail: alekhyapatel4a4@gmail.com

Abstract— Electro-encephalogram (EEG) is the electrical activity of brain cell groups in the cerebral cortex or the scalp surface. It plays an important role in studying the patient mental condition and Human Machine interfacing. Normal EEG signals can avail in the band of DC to 60 Hz frequencies with a few hundreds of micro volts of strength. Ocular artifacts and muscular noise with similar statistical properties are the major challenges which make the analysis more complex and may yields wrong interpretation. Here in this paper we discussed various thresholding techniques in the removal of ocular artifacts (OA) present in the EEG signal and there by compared performance these thresholding techniques in the removal of OA's with the help of various statistical parameters. In this paper the collected EEG signal is decomposed to 4 levels using db10 and sym8 wavelets and later threshold the detail coefficients using various thresholding techniques and estimated the statistical parameters of it.

Keywords— EEG, EOG, Ocular artifacts and Wavelet transform.

I. Introduction

Electrooculography (EOG) artifacts inevitably and frequently interfere with the electroencephalogram (EEG) signals. Eye-movement and eye-blink artifacts are the main sources of ocular artifacts. The frequency components of EEG signals are in the order of just a few up to 200 μ V, and their frequency content differs among the different neurological rhythms, such as, alpha, beta, delta and theta rhythms [1]. However, artifacts and noise are the outstanding enemies of high quality EEG signals. Their presence is thus crucial for the accurate evaluation of EEG signal. They fall into two major categories: technical and physiological artifacts. The technical artifacts are often found in power line noise 50/60Hz results from poor electrode application on the scalp and transducer's artifacts. The physiological artifacts are often due to ocular, heart and muscular activity; are the EMG, EOG and ECG artifacts respectively [2].

To date, many method are presented to remove EOG artifacts.. Some methods based on regression in the time domain or frequency domain [3-5] is proposed for removing eye blink artifacts. However, they always need a reliable reference channel. Moreover, EOG Reference channel often contains brain signals which will be also removed inevitably from the EEG by the procedure of regression. Therefore, the methods based on regression may not be the best way to remove EOG artifacts.

In this study, the EEG signal is decomposed into a level 4, which gives us approximate and detail coefficients. The detail coefficients which are having more noise information are processed with various thresholding techniques and later estimated the statistical parameters.

The noisy EEG signal is convolved with a low and high pass filter whose impulse response is determined by the wavelet chosen. The output of each filter produces the same number of samples as the original signal, so both outputs are down sampled by 2 resulting in the Approximate and detail coefficients each with half the number of points as that of the original signal.

The coefficients represent a correlation between the signal of interest and wavelet chosen at different scales and during translation. Because all of the coefficients are preserved, the original signal or any level of decomposition can be reconstructed using a filter scheme similar to decomposition shown in Figure 1. The process is reversed and now the coefficients are up sampled (interpolated), filtered, and summed.

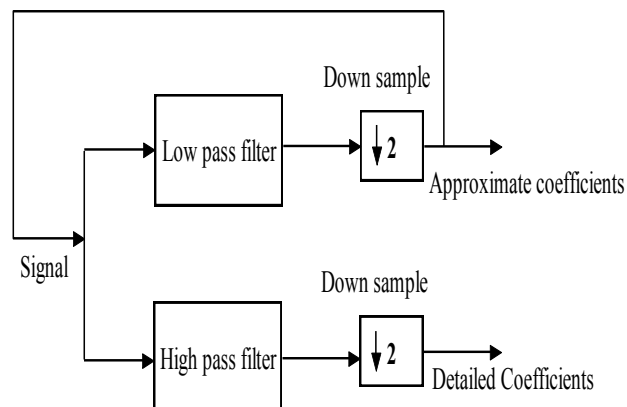


Figure.1. Block diagram to show DWT decomposition

The EEG signal is decomposed into 4 levels using dB10 and Sym8 wavelets and corresponding approximate and detail coefficients. From derived coefficients high frequency components will be distributed in approximate coefficients and low frequency components presents in Detail coefficients cD4, cD3, cD2, cD.

II. WAVELET TRANSFORM

A wavelet transform is the representation of a function by wavelets. The wavelets are scaled and translated copies (known as "daughter wavelets") of a finite-length or fast-decaying oscillating waveform (known as the "mother wavelet"). Wavelet transforms have advantages over traditional Fourier transforms for representing functions that have discontinuities and sharp peaks, and for accurately deconstructing and reconstructing finite, non-periodic and/or non-stationary signals.

Wavelet Transform can be represented as a linear transformation i.e. $Y = WX$, where X , Y are input and output of the transformation and W is orthogonal mother wavelet transformation matrix. Mother wavelet is defined as

$$\psi_{u,s}(t) = \frac{1}{\sqrt{s}} \psi\left(\frac{t-u}{s}\right) \quad (1.1)$$

Wavelets are oscillating functions of time that must satisfy several conditions: A wavelet ψ has zero time average and unit energy corresponds to orthonormality property of wavelets. The amplitudes of a wavelet have large fluctuations within a designated time period and extremely small values outside of that time while being band-limited in terms of their frequency content. The CWT of a signal $f(t)$ can be calculated using equation

$$F(u,s) = \int f(t) \frac{1}{\sqrt{s}} \psi^*\left(\frac{t-u}{s}\right) dt \quad (1.2)$$

By varying the values for s and u results in an infinite number of combinations, can be used to decompose the signal $f(t)$. Here u and s are the translation and dilation respectively.

A much more computationally efficient approach is the use of the discrete wavelet transform (DWT), which was developed by Mallat. Knowing only the values of the DWT coefficients, the waveform can be perfectly reconstructed. All of the extra coefficients of the CWT create a redundancy in calculation because they are highly correlated with the ones of the DWT. In implementation, the DWT performs even better because waveforms are already digitally sampled and have finite duration so the number of coefficients is limited DWT or CWT can be seen as a number on the time scale plane representing the correlation between the *signal* vector and the wavelet function at a given time-scale point. The DWT produces as many wavelet coefficients as there are samples in the noisy EEG signal by using a filter scheme shown in Fig. 1.

III. METHODOLOGY

The EEG and EOG data sets are collected from Physionet data base[6]. The collected EEG and EOG signals were normalized by subtracting the mean and later divided by the standard deviation. The EEG signal is mixed with the EOG signal to obtain a noisy EEG signal. The noisy EEG signal is convolved with a low and high pass filter whose impulse response is determined by the wavelet chosen. The output of each filter produces the same number of samples as the original signal, so both outputs are down sampled by 2 resulting in the approximation and detail coefficients each with half the number of points as the original signal.

The EEG signal will be corrupted by ocular artifacts during the process of signal acquisition. The corrupted EEG signal (observed) is given as

$$y = y_i = s_i + v_i \quad i = 1, \dots, n. \quad (1.3)$$

Where s_i is original EEG signal, v_i represents the EOG signal with variance $N(0, \sigma^2)$ here the problem is to remove or attenuate the maximum no. of v_i from the output signal 'y'.

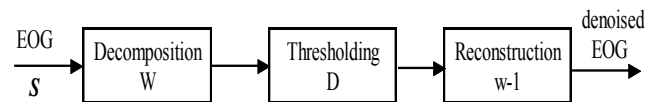


Figure 2. Wavelet denoising

Noisy corrupted signal is decomposed into 4 levels with all the mother wavelets. The sub bands thus formed contains the frequencies in the bands of 0-10 Hz, 10-20 Hz, 20-40 Hz and 40-80 Hz. These sub bands contains almost all the energy contained by the signal. Since the mother wavelet resembles the signal's and large coefficients are generated corresponding to the eye moments and low coefficients corresponding to the noise. Various thresholding techniques such as Heursure, Rigrsure, minimaxi, and sqtwolog[6] along with soft and hard thresholding.

- Soft thresholding:

$$y = \text{sgn}(x) \cdot (|x| - th) \quad |x| \geq th \\ = 0 \quad |x| \leq th \quad (1.4)$$

- Hard thresholding:

$$y = x \quad |x| \geq th \\ = 0 \quad |x| \leq th \quad (1.5)$$

One of the sample results obtained using one of the thresholding technique namely Heursure –hard thresholding technique using matlab [7] are shown in the Figure 3. The process is repeated using Rigrsure, minimaxi and sqtwolog thresholding techniques using dB10 and Sym8 wavelets and the results are tabulated in the table 1.1 and table 1.2 respectively.

Table 1.1 Statistical parameters of EEG signal obtained using dB10 with various thresholding techniques

Parameters/ wavelet and thresholding	dB10							
	Heursure (h)	Heursure (s)	Rigrsure (h)	Rigrsure (s)	Minimax i (h)	Minimax x (s)	Sqtwolog (h)	Sqtwolog(s)
Mean Square Error	0.0937	0.1094	0.0453	0.0670	0.0701	0.0877	0.1179	0.2283
Mean Absolute Error	0.2365	0.2554	0.1609	0.2028	0.1974	0.2167	0.2650	0.3647
Signal to Noise Ratio (dB)	10.2705	9.5973	13.4237	11.7258	11.5309	10.5611	9.2730	6.4054
Peak Signal to Noise Ratio(dB)	17.6678	16.9946	20.8210	19.1231	22.0915	21.1218	16.6703	13.8027
Correlation Coefficient	0.9519	0.9440	0.9770	0.9667	0.9643	0.9551	0.9390	0.8790

Table 1.2 Statistical parameters of EEG signal obtained using sym8 with various thresholding techniques

Parameters/ wavelet and thresholding	Sym8							
	Heursure (h)	Heursure (s)	Rigrsure (h)	Rigrsure (s)	Minimax i (h)	Minimax xi (s)	Sqtwolog (h)	Sqtwolog(s)
Mean Square Error	0.0820	0.0961	0.0406	0.0403	0.0636	0.1109	0.1179	0.1870
Mean Absolute Error	0.2210	0.2375	0.1564	0.1558	0.1961	0.2635	0.2650	0.3349
Signal to Noise Ratio (dB)	10.8515	10.1611	13.9012	13.9423	11.9549	9.5412	9.2730	7.2714
Peak Signal to Noise Ratio(dB)	18.2488	17.5584	21.2985	22.2340	19.3522	16.9385	16.6703	14.6687
Correlation Coefficient	0.9580	0.9508	0.9794	0.9796	0.9676	0.9439	0.9390	0.9018

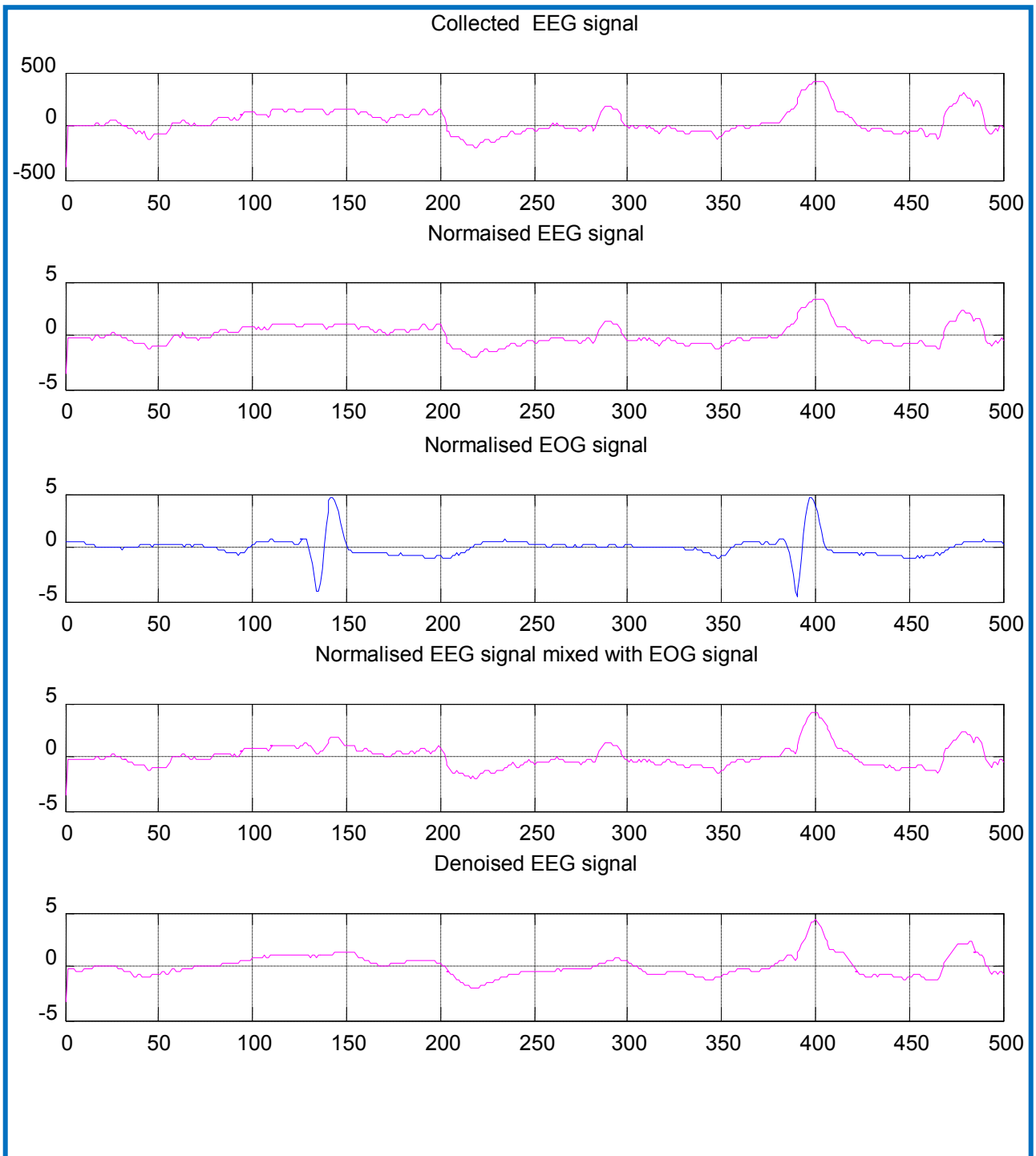


Figure 3. Collected, Noisy and Denoised EEG Signal Using Heursure-Hard Thresholding

IV CONCLUSION

The noisy EEG signal is processed with dB10 and Sym8 wavelets using Heursure, Rigrsure, minimaxi and sqtwolog thresholding techniques and later estimated the various Statistical parameters of EEG signal. From the Table 1.1 and Table 1.2, it is observed that the better results obtained in the denoising process of noisy EEG signal using dB10 wavelet with the help of Rigrsure-hard thresholding technique, providing better SNR of 13.4237dB, PSNR of 20.8210 dB , MSE of 0.0453 and Correlation Coefficient of 0.9770.

In case of sym8 wavelet the better results obtained in the denoising process of noisy EEG signal with the help of Rigrsure-soft thresholding technique, providing better SNR of 13.9423 dB, PSNR of 22.2340 dB , MSE of 0.0403 and Correlation Coefficient of 0.9796.

The originality of the signal is not going to be affected by the decomposition of EEG signal and the noise can be reduced considerably using Sym8 wavelet with the help of Rigrsure-soft thresholding.

In order to process the noisy EEG signal for the removal of OA, the Sym8 wavelet with the help of Rigrsure- soft thresholding providing better results than dB10.

REFERENCES

- [1]. N.V. Thakor et al. (1993). "Multi resolution Wavelet Analysis of Evoked Potentials", IEEE Transactions on Biomedical Engineering, Vol. 40, No 11, pp. 1085-1093, November.
- [2]. S. Ventakaramanan, P. Prabhat, S.R Choudhury, H.B Nemade, and J.S. Sahambi. (2000). "Biomedical Instrumentation Based On Electrooculogram (EOG) Signal Processing And Application To A Hospital Alarm System", Indian Institute Of Technology (IIT) Gunawati, Proceedings of IEEE ICISEP, pp.535-539.
- [3] Schlogl A, Keinrath C, Zimmermann D et al. 2007. A fully automated correction method of EOG artifacts in EEG recordings. *Clinical Neurophysiology*.118, 98–104.
- [4] Jung T-P, Makeig S, Humphries C, Lee T-W, McKeown MJ, Iragui V and Sejnowski TJ. 2000a. Removing Electroencephalographic artifacts by blind source separation. *Psychophysiology*.37, 163 –178.
- [5] Gratton G, Coles MG and Donchin E. 1983. A new method for off-line removal of ocular artifact. *Electroencephalography Clin.Neurophysiol*. 55, 484– 486.
- [6] www.physionet.org
- [7] Mathworks.com



Certificate of Publication

This is to certify that

Ms. Lavanya Pamulaparty

Assoc. professor

Department of Computer Science and Engineering
Methodist College of Engineering and Technology, Hyderabad,
India-500085

has published a paper titled

**A Gradient Boosting Approach for Large-Scale Network
Parameter Configuration in Bigdata**

in the First International Conference on
Recent Innovations in Engineering and Technology (ICRIEAT-2016)

Organized by

Aurora's Scientific, Technological and Research Academy
Chandrayangutta, Hyderabad - 500 005
held on 22 & 23 December 2016.

A handwritten signature in blue ink, appearing to read 'Pradosh Chandra Patnaik'.

Pradosh Chandra Patnaik
Conference Vice Chair

A handwritten signature in black ink, appearing to read 'Srilatha Chepure'.

Srilatha Chepure
Conference General Chair